Anderson transition on the Cayley tree
as a traveling wave critical point for various probability distributions

Cécile Monthus and Thomas Garel

Institut de Physique Théorique, CNRS and CEA Saclay 91191 Gif-sur-Yvette cedex, France

For Anderson localization on the Cayley tree, we study the statistics of various observables as a function of the disorder strength W and the number N of generations. We first consider the Landauer transmission T_N. In the localized phase, its logarithm follows the traveling wave form $\ln T_N \simeq \overline{\ln T_N} + \ln t^*$ where (i) the disorder-averaged value moves linearly $\overline{\ln(T_N)} \simeq -\frac{N}{\xi_{loc}}$ and the localization length diverges as $\xi_{loc} \sim (W - W_c)^{-\nu_{loc}}$ with $\nu_{loc} = 1$ (ii) the variable t^* is a fixed random variable with a power-law tail $P^*(t^*) \sim 1/(t^*)^{1+\beta(W)}$ for large t^* with $0 < \beta(W) \leq 1/2$, so that all integer moments of T_N are governed by rare events. In the delocalized phase, the transmission T_N remains a finite random variable as $N \to \infty$, and we measure near criticality the essential singularity $\overline{\ln(T_\infty)} \sim -|W_c - W|^{-\kappa_T}$ with $\kappa_T \sim 0.25$. We then consider the statistical properties of normalized eigenstates $\sum_x |\psi(x)|^2 = 1$, in particular the entropy $S = -\sum_x |\psi(x)|^2 \ln |\psi(x)|^2$ and the Inverse Participation Ratios (I.P.R.) $I_q = \sum_x |\psi(x)|^{2q}$. In the localized phase, the typical entropy diverges as $S_{typ} \sim (W - W_c)^{-\nu_S}$ with $\nu_S \sim 1.5$, whereas it grows linearly $S_{typ}(N) \sim N$ in the delocalized phase. Finally for the I.P.R., we explain how closely related variables propagate as traveling waves in the delocalized phase. In conclusion, both the localized phase and the delocalized phase are characterized by the traveling wave propagation of some probability distributions, and the Anderson localization/delocalization transition then corresponds to a traveling/non-traveling critical point. Moreover, our results point towards the existence of several length scales that diverge with different exponents ν at criticality.

I. INTRODUCTION

Since its discovery fifty years ago [1] Anderson localization has remained a very active field of research (see for instance the reviews [2–7]). According to the scaling theory [8], there is no delocalized phase in dimensions $d = 1, 2$, whereas there exists a localization/delocalization at finite disorder in dimension $d > 2$. To get some insight into this type of transition, it is natural to consider Anderson localization on the Cayley tree (or Bethe lattice) which is expected to represent some mean-field limit. The tight-binding Anderson model on the Cayley tree has been thus studied by various authors. In [9], the recursion equation for the self-energy has been studied to establish the mobility edge as the limit of stability of localized states. In [10], the exponent ν governing the divergence of the localization length was shown to be $\nu = 1$. In [11], the supersymmetric formalism has been used to predict the critical behavior of some disorder-averaged observables (see also [12–15] where similar results have been obtained for the case where Anderson tight-binding model is replaced by a non-linear σ-model). In [16, 17], the problem was reformulated in terms of recursions on Riccati variables to obtain weak-disorder expansions. Other studies have focused on random-scattering models on the Cayley tree [18–20]. More recently, the interest in Anderson localization on the Cayley tree has been revived by the question of many-body localization [21], because the geometry of the Fock space of many-body states was argued to be similar to a Cayley tree [22–25].

In the present paper, we consider the Anderson tight binding model on the Cayley tree already studied in [9–11, 16, 17] and we study numerically the statistical properties of Landauer transmission and eigenstates as a function of the disorder strength W and of the number N of generations. We find that several probability distributions propagate as traveling waves with a fixed shape, as the number N of tree generations grows. The fact that traveling waves appear in disordered models defined on trees has been discovered by Derrida and Spohn [26] on the specific example of the directed polymer in a random medium and was then found in various models [27]. For the case of Anderson localization on trees, the analysis of [9] concerning the distribution of the self-energy in the localized phase is actually a 'traveling wave analysis' (see Appendix A for more details), although it is not explicitly mentioned in these terms in [9]. The fact that traveling waves occur has been explicitly seen in the numerical study of the transmission distribution for a random-scattering model on the Cayley tree (see Fig. 8b of [20]) and has been found within the supersymmetric formalism [12, 14, 15]. In the field of traveling waves and front propagation (see the reviews [28, 29]), there exists an essential separation between two classes : in 'pulled fronts', the velocity is determined by the form of the tail of the front and thus by the appropriate linearized equation in the tail region, whereas in 'pushed fronts', the velocity is determined by the bulk properties and thus by the non-linear dynamics in the bulk region. It turns out that for disordered systems defined on trees, the traveling waves that appear usually correspond to cases where it is the tail of the probability distribution that determines the velocity [26]. In particular for Anderson localization on the Cayley tree, the traveling wave propagation is also determined by the tails [9]. From this traveling wave point

of view, the localization/delocalization Anderson transition thus represents a traveling/non-traveling critical point. Such a traveling/non-traveling phase transition for a branching random walk in the presence of a moving absorbing wall has been studied recently in [30] and we find here very similar behaviors in the critical region.

The paper is organized as follows. In Section II, we describe the statistical properties of Landauer transmission. In Section III, we discuss the statistical properties of eigenstates, as measured by the entropy and Inverse Participation Ratios (I.P.R.). We summarize our conclusions in Section IV. In Appendix A, we translate the analysis of Ref. [9] concerning the distribution of the self-energy in the localized phase into a traveling-wave tail analysis for the Landauer transmission discussed in section II. In Appendix B, we explain how such a similar tail analysis can be performed in the delocalized phase for auxiliary variables that are closely related to Inverse Participation Ratios. Finally, in Appendix C, we recall the results of Ref. [30] concerning the traveling/non-traveling phase transition for a branching random walk in the presence of a moving absorbing wall, since these results are used as a comparison in the text to understand the finite-size scaling properties in the critical region.

II. STATISTICAL PROPERTIES OF THE LANDAUER TRANSMISSION

In quantum coherent problems, the most appropriate characterisation of transport properties consists in defining a scattering problem where the disordered sample is linked to incoming wires and outgoing wires and in studying the reflexion and transmission coefficients. This scattering theory definition of transport, first introduced by Landauer [31], has been much used for one-dimensional systems [32–34] and has been generalized to higher dimensionalities and multi-probes measurements (see the review [35]). In dimension $d = 1$, the transfer matrix formulation of the Schrödinger equation yields that the probability distribution of the Landauer transmission becomes asymptotically log-normal [32, 34] , i.e. one has

$$\ln T_L^{(1d)} = -\frac{L}{\xi_{loc}} + L^{1/2}u \tag{1}$$

where ξ_{loc} represents the localization length and where u is a sample-dependent random variable of order $O(1)$ distributed with a Gaussian law. Although it is often assumed that this log-normal distribution persists in the localized phase in dimension $d = 2, 3$, recent numerical studies [36] are in favor of the following scaling form for the logarithm of the conductance

$$\ln g_L^{(d)} = -\frac{L}{\xi_{loc}} + L^{\omega(d)}u \tag{2}$$

with exponents of order $\omega(d = 2) \simeq 1/3$ and $\omega(d = 3) \simeq 1/5$ [36], whereas $\omega(d = 1) = 1/2$ from Eq. 1. For the Cayley tree that we consider in this paper, we will find below that the fluctuation exponent vanishes $\omega_{Cayley} = 0$, and we will discuss the probability distribution of the variable u. But let us first recall the appropriate scattering framework for the Cayley tree [17] .

A. Reminder on the Miller-Derrida framework to compute the Landauer transmission [17]

We consider the Anderson tight-binding model

$$H = \sum_i \epsilon_i |i><i| + \sum_{<i,j>} |i><j| \tag{3}$$

where the hopping between nearest neighbors $< i, j >$ is a constant $V = 1$ and where the on-site energies ϵ_i are independent random variables drawn from the flat distribution

$$p(\epsilon_i) = \frac{1}{W}\theta\left(-\frac{W}{2} \leq \epsilon_i \leq \frac{W}{2}\right) \tag{4}$$

The parameter W thus represents the disorder strength.

We consider the scattering geometry introduced in [17] and shown on Fig. 1 : the finite tree of branching ratio K is attached to one incoming wire at its root (generation $n = 0$) and to K^{2N} outgoing wires at generation $2N$. One is interested into the eigenstate $|\psi >$ that satisfies the Schrödinger equation
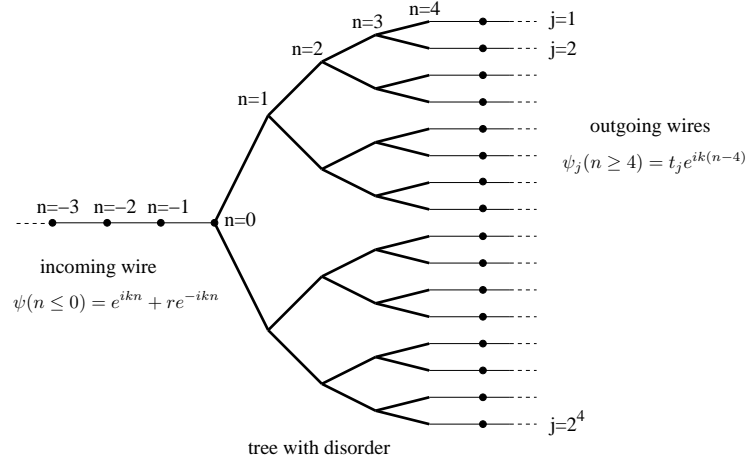
$$H|\psi >= E\psi > \tag{5}$$

FIG. 1: Scattering geometry of Ref. [17] : the disordered tree of branching ratio $K = 2$ starting at generation $n = 0$ and ending at generation $2N$ (on the Figure $2N = 4$) is attached to one incoming wire and to K^{2N} outgoing wires. In section II, we discuss the properties of the total transmission $T \equiv \sum_j |t_j|^2 = 1 - |r|^2$ where r is the reflexion amplitude of the incoming wire, and t_j the transmission amplitudes of the outgoing wires.

inside the disorder sample and in the wires where one requires the plane-wave forms

$$
\begin{aligned}
\psi(n \leq 0) &= e^{ikn} + re^{-ikn} \\
\psi_j(n \geq 2N) &= t_j e^{ik(n-2N)}
\end{aligned}
\tag{6}
$$

These boundary conditions define the reflexion amplitude r of the incoming wire and the transmission amplitudes t_j of the $j = 1, 2, ..K^{2N}$ outgoing wires. To satisfy the Schrödinger Equation of Eq. 5 within the wires with the forms of Eq. 6, one has the following relation between the energy E and the wave vector k

$$
E = 2\cos k
\tag{7}
$$

To simplify the discussion, we will focus in this paper on the case of zero-energy $E = 0$ and wave-vector $k = \pi/2$

$$
\text{In this paper :} \quad E = 0 \quad \text{and} \quad k = \pi/2
\tag{8}
$$

because the zero-energy $E = 0$ corresponds to the center of the band where the delocalizion first appears when the strength W of the disorder is decreased from the strong disorder localized phase.

Inside the Cayley tree $0 \leq n \leq 2N - 1$, the Schrödinger Equation of Eq. 5 involves one ancestor denoted by $anc(n, j)$ and K descendants denoted by $des_m(n, j)$

$$
0 = \epsilon(n, j)\psi(n, j) + \psi(anc(n, j)) + \sum_{m=1}^{K} \psi(des_m(n, j))
\tag{9}
$$

whereas for the last generation $2N$ there is only one ancestor and one descendant (outgoing wire)

$$
0 = \epsilon(2N, j)\psi(2N, j) + \psi(anc(2N, j)) + \psi(2N + 1, j)
\tag{10}
$$

As explained in [17], it is convenient to introduce the Riccati variables

$$
R(n, j) \equiv \frac{\psi(anc(n, j))}{\psi(n, j)}
\tag{11}
$$

that represent the ratio of the wave function of two neighboring sites. On the outgoing wires, these Riccati variables are fixed by Eq. 6 to be

$$
R(2N + 1, j) = \frac{\psi(2N, j)}{\psi(2N + 1, j)} = e^{-ik} = -i
\tag{12}
$$

The Schrödinger equation of Eq. 10 gives the first recursion

$$R(2N, j) = -\epsilon(2N, j) - \frac{1}{R(2N+1, j)} = -\epsilon(2N, j) - e^{ik} = -\epsilon(2N, j) - i \tag{13}$$

whereas the Schrödinger equation of Eq. 9 gives the recursion inside the tree for $0 \le n \le 2N - 1$

$$R(n, j) = -\epsilon(n, j) - \sum_{m=1}^{K} \frac{1}{R(des_m(n, j))} \tag{14}$$

On the other hand, the value of the Riccati variable for the origin of the tree $n = 0$ is fixed by the incoming wire of Eq. 6

$$R(0) = \frac{\psi(-1)}{\psi(0)} = \frac{e^{-ik} + re^{ik}}{1 + r} \tag{15}$$

and thus the reflexion coefficient r can be obtained via

$$r = -\frac{R(0) - e^{-ik}}{R(0) - e^{ik}} = \frac{i + R(0)}{i - R(0)} \tag{16}$$

from the $R(0)$ obtained via the recursion of Eq. 14. From the conservation of energy, the total transmission T is related to the reflexion coefficient $|r|^2$

$$T \equiv \sum_j |t_j|^2 = 1 - |r|^2 \tag{17}$$

As explained in [17], the criterion for the localization/delocalization phases is then the following :

(a) if the Riccati variable $R(0)$ at the root of the tree converges towards a real random variable as $N \to \infty$, the reflexion is total $|r| = 1$ and the transmission vanishes $T = 0$.

(b) if the Riccati variable $R(0)$ keeps a finite negative imaginary part as $N \to \infty$, the reflexion is only partial $|r| < 1$ and the transmission remains finite $T = 1 - |r|^2 > 0$

We refer to [17] for the results of a weak disorder expansion within this framework, and for a numerical Monte-Carlo approach to determine the mobility edge in the plane (E, W). Here we will instead study the statistical properties of the transmission T at zero energy $E = 0$ as a function of the disorder strength W (Eq 4) and of the number N of generations. But before discussing the disordered case, let us first describe the finite-size properties of the pure case.

B.   Example : transmission of finite pure trees

In the pure case where all on-site energies vanish $\epsilon(n, j) = 0$, all branches are equivalent and there is no dependence on j. The recursions for Riccati variables of Eqs 12, 13 and 14 give

$$\begin{aligned} R_{pure}(2N+1) \quad &= -i \\ R_{pure}(2N) \quad &= -i \\ R_{pure}(n) \quad &= -\frac{K}{R_{pure}(n+1)} \quad \text{for} \ \ 0 \le n \le 2N - 1 \end{aligned} \tag{18}$$

i.e. one obtains the simple alternation between odd and even generations

$$\begin{aligned} R_{pure}(2N-1) \quad &= -\frac{K}{R_{pure}(2N)} = -Ki \\ R_{pure}(2N-2) \quad &= -\frac{K}{R_{pure}(2N-1)} = -i \\ \dots \quad &\dots \\ R_{pure}(1) \quad &= -Ki \\ R_{pure}(0) \quad &= -i \end{aligned} \tag{19}$$

$$\tag{20}$$

The reflexion coefficient r thus vanishes exactly for any even size $(2N)$

$$r_{pure} = \frac{i + R_{pure}(0)}{i - R_{pure}(0)} = 0 \tag{21}$$

and the transmission coefficient in each branch $j = 1, .., K^{2N}$ reads

$$t_j^{pure} = (1 + r) \prod_{n=1}^{2N} \frac{1}{R_{pure}(n)} = \frac{1}{(-K)^N} \tag{22}$$

(Note that for pure trees of uneven size, the reflexion would not vanish. This is why in the disordered case, we will only consider trees of even sizes $2N$ where in the corresponding pure case, the reflexion vanish exactly for any finite tree). It is instructive to write now the corresponding wave function as a function of the generation n,

$$
\begin{aligned}
\ldots \quad \psi_{pure}(-4) \quad &= 1 \\
\psi_{pure}(-3) \quad &= i \\
\psi_{pure}(-2) \quad &= -1 \\
\psi_{pure}(-1) \quad &= -i \\
\psi_{pure}(0) \quad &= 1 \\
\psi_{pure}(1) \quad &= \frac{i}{K} \\
\psi_{pure}(2) \quad &= -\frac{1}{K} \\
\psi_{pure}(3) \quad &= -\frac{i}{K^2} \\
\psi_{pure}(4) \quad &= \frac{1}{K^2} \quad \ldots
\end{aligned}
\tag{23}
$$

This exponential decay of the wavefunction in this delocalized case is very peculiar to the tree geometry : it is imposed by the energy conservation and by the exponential growth of the number of sites with the generation n.

C. Statistics over the disordered samples of the transmission T_N

1. Numerical pool method

If one wishes to study numerically real trees, one is limited to rather small number of generations of order $N_{max} \sim 12, 14$ (see for instance the study [37] based on exact diagonalization) because the number of sites and thus of random energies grows exponentially in N. From the point of view of convergence towards stable probability distributions via recursion relations, it is thus better to use the so-called 'pool method' that will allow us to study much larger number of generations (see below Eq. 27). The idea of the pool method is the following : at each generation, one keeps the same number M_{pool} of random variables to represent probability distributions. Within our present framework, the probability distribution $P_n(R)$ of the Riccati variables R at generation n will be represented by a pool of M_{pool} complex values $\{R_n^{(1)}, .., R_n^{(M_{pool})}\}$. It is convenient from now on to change the notation $n \to 2N - n$ with respect to Fig. 1 so that $n = 0$ now corresponds to the contacts with the outgoing wires (see Fig. 1). The numerical results presented below have been obtained with the following procedure :

(i) the random variables of the initial pool are given by (Eq. 13)

$$R_0(j) = -\epsilon_0(j) - i \tag{24}$$

where $\epsilon(j)$ are independent random variables drawn with Eq. 4.

(ii) From the random variables $R_{n-1}(j)$ of the pool at generation $n - 1$, the pool at generation n is constructed as follows. For each $j = 1, 2, .. M_{pool}$, one generates a new random energy $\epsilon_n(j)$ with the law of Eq. 4 and one draws K random indices $\{j_1(j), .. j_K(j)\}$ among the pool of generation $(n - 1)$ to construct the variable $R_n(j)$ as follows(Eq. 14)

$$R_n(j) = -\epsilon_n(j) - \sum_{m=1}^{K} \frac{1}{R_{n-1}(j_m(j))} \tag{25}$$

(iii) From these pools of Riccati variables, one may compute via Eqs 16 and 17 a pool of total transmission $T_n(j)$ for trees of n generations using

$$T_n(j) = 1 - |r_n(j)|^2 = 1 - \left|\frac{i + R_n(j)}{i - R_n(j)}\right|^2 \tag{26}$$

For the Anderson model on the Bethe lattice, the pool method has been already used, in particular in [9] with a pool $M_{pool} = 1800$ with a number $N_{max} \sim 30$ of generations, in [17] with pools up to $M_{pool} = 10000$, and in [20] with pools up to $M_{pool} = 16384$ with a number $N_{max} \sim 400$ of generations. The pool method is also very much used for disordered systems on hierarchical lattices (see for instance[38–40]),

In the remaining of this section, we present the numerical results obtained with a pool of size

$$M_{pool} = 10^5 \quad \text{with a number of generations} \quad N \leq N_{max} = 34.10^5 \tag{27}$$

We have also results for a pool of size $M_{pool} = 10^6$ with a number of generations $N \leq N_{max} = 24.10^4$ to see how the results change with the pool size. However, the number of generations N_g for this bigger pool $M_{pool} = 10^6$ has turned out to be less precise in the critical region. All figures shown below thus corresponds to data obtained with the pool of size $M_{pool} = 10^5$.

As is usual with the pool method [40], the location of the critical point depends on the pool, i.e. on the discrete sampling with M_{pool} values of probability distributions. It is expected to converge towards the thermodynamic critical point only in the limit $M_{pool} \to \infty$ (see the discussion of section B 3 in Appendix B). Nevertheless, for each given pool, the critical behaviors with respect to this pool-dependent critical point usually allows a good measure of critical exponents [40]. For instance, for the pool of size $M_{pool} = 10^5$, the critical value W_c of the disorder strength where the localization-delocalization occurs for the Landauer transmission is of order

$$W_c(M_{pool} = 10^5) \simeq 16.99.. \tag{28}$$

For the pool of size $M_{pool} = 10^6$, we find that it is higher and of order $W_c(M_{pool} = 10^6) \simeq 17.32...$ This rather important shift of the pseudo-critical point with the pool size which has already been seen in [17], seems to be due to the very slow logarithmic convergence of traveling wave velocity in the presence of cut-off (see the discussion of section B 3 in Appendix B). So we stress that here, in contrast to [9, 17], our goal is not to determine the true thermodynamic mobility edge $W_c(+\infty)$, but instead to understand the critical behaviors of the finite-pool results with respect to the pool-dependent critical point of Eq. 28.

We will first discuss the behavior of the typical transmission T_N^{typ} defined by

$$\ln(T_N^{typ}) \equiv \overline{\ln T_N} \tag{29}$$

as a function of the number N of generations and disorder strength W, before we turn to the distribution around this typical value.

2. Exponential decay of the typical transmission T_N^{typ} in the localized phase $W > W_c$

In the localized phase, one expects that the typical transmission T_N^{typ} defined by Eq. 29 decays exponentially with the number N of generations

$$\ln(T_N^{typ}) \equiv \overline{\ln T_N(W > W_c)} \underset{N \to \infty}{\simeq} -\frac{N}{\xi_{loc}(W)} \tag{30}$$

where ξ_{loc} represents the localization length that diverges at the delocalization transition

$$\xi_{loc}(W) \underset{W \to W_c^+}{\simeq} (W - W_c)^{-\nu_{loc}} \tag{31}$$

.

We show on Fig. 2 our numerical results for the pool of size $M_{pool} = 10^5$ (Eq. 27) : the exponential decay with N of Eq. 30 is shown on Fig. 2 (a) for various disorder strength W. The corresponding slope $1/\xi_{loc}(W)$ is shown as a function of W on Fig. 2 (b) : we find that this slope vanishes linearly in $(W - W_c)$, in agreement with the exact result [10, 11]

$$\nu_{loc} = 1 \tag{32}$$

and in agreement with Figure 7 of Ref. [20] concerning a random-scattering model on the Cayley tree.
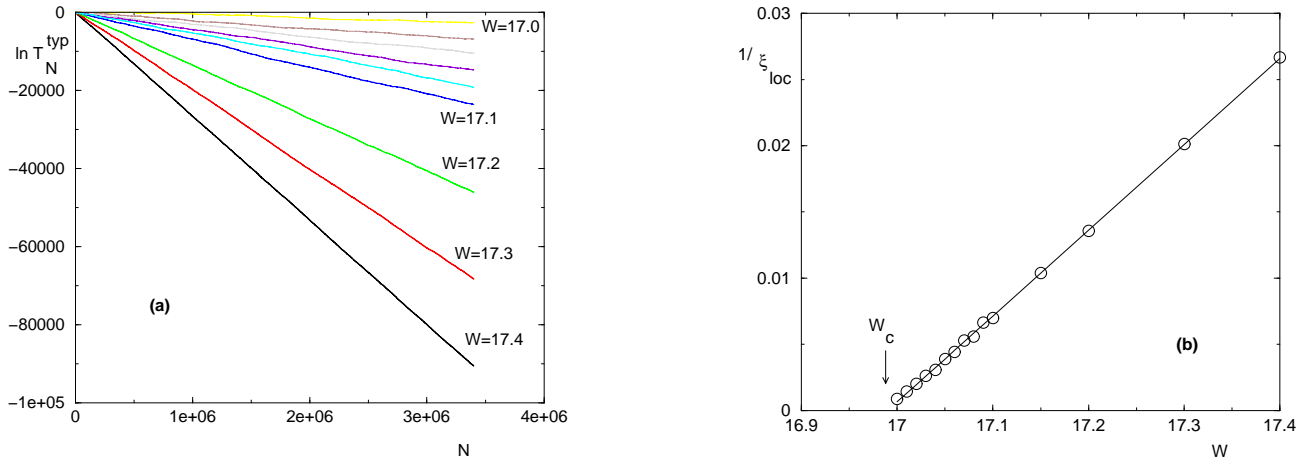
FIG. 2: Exponential decay of the typical transmission $T_N^{typ} \equiv e^{\overline{\ln T_N}}$ in the localized phase $W > W_c$: (a) Linear decay of $\overline{\ln T_N}$ as a function of the number N of generations (see Eq. 30). (b) Behavior of the slope $1/\xi_{loc}(W)$ as a function of the disorder strength W : it vanishes linearly $1/\xi_{loc}(W) \sim (W - W_c^{pool})^{\nu_{loc}}$ with $W_c^{pool} \simeq 16.99$ (see Eq. 28) and $\nu_{loc} = 1$ (see Eq. 31)

3. Behavior of the typical transmission T_∞^{typ} in the delocalized phase $W < W_c$ near criticality
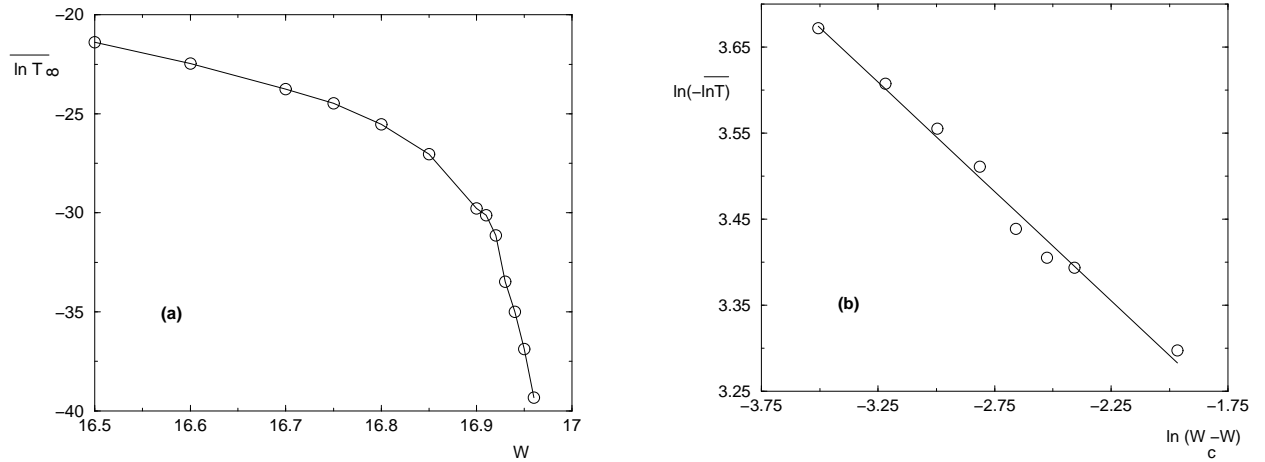

FIG. 3: Behavior of the typical transmission T_∞^{typ} of the infinite tree in the delocalized phase : (a) $\ln T_\infty^{typ} \equiv \overline{\ln T_\infty(W < W_c)}$ as a function of the disorder strength W (b) same data in a log-log plot to measure the exponent of the essential singularity of Eq. 34 : $\ln(-\ln T_\infty^{typ})$ as a function of $\ln(W_c - W)$: the slope is of order $\kappa_T \sim 0.25$

In the delocalized phase, the typical transmission remains finite in the limit where the number of generations N diverges

$$\overline{\ln T_N(W < W_c, N)} \underset{N \to \infty}{\simeq} \overline{\ln T_\infty(W < W_c)} > -\infty \tag{33}$$

As shown on Fig. 3, we measure the following essential singularity behavior of the typical transmission

$$\overline{\ln T_\infty(W < W_c)} \underset{W \to W_c^-}{\simeq} -(W_c - W)^{-\kappa_T} \quad \text{with} \quad \kappa_T \sim 0.25 \tag{34}$$

The presence of essential singularities in transport properties near the localization transition on the Bethe lattice has been found in [11] via the supersymmetric formalism (see also [12–15] where similar results have been obtained for the case where Anderson tight-binding model is replaced by a non-linear σ-model). In particular, Eq. 71 of Ref. [11]) states that the leading critical behavior of the diffusion constant is given by : $\ln \mathcal{D} \sim -|E - E_c|^{-1/2}$ (Eq. 71 of Ref. [11]). We note that the exponent in this essential singularity is $1/2$ instead of the exponent of order $1/4$ that we measure. The reason for this difference could be that the results of Ref. [11] are based on the computation of the

disorder-averaged two-point density-density correlation function (see Eq. 2 of Ref. [11]), whereas our numerical results concern the *typical value of Landauer transmission*, and not the disorder-averaged transmission which is expected to be governed by rare events (see below the section II C 5). Also it is not clear to us what exactly represents the diffusion constant computed in [11], because it is known that on the Bethe lattice the dynamics is not diffusive but ballistic in the delocalized phase [41], and that more generally the random walk on the Bethe lattice is not diffusive because the tree-geometry induces an effective bias away from the origin (see for instance [42] and references therein). As a consequence, some implicit reinterpretation of the Bethe lattice seems to underlie the statements of Ref. [11] that makes difficult a precise comparison with our present numerical results.

4. Finite-size scaling in the critical region

If there exists some finite-size scaling in the critical region for the typical Landauer transmission of the form

$$\overline{\ln T_N(W)} \simeq -N^{\rho_T} G\left(N^{1/\nu_T^{FS}}(W_c - W)\right) \tag{35}$$

the matching of our results in the localized phase (see Eq. 30) and in the delocalized phase (Eq. 34) requires a finite-size correlation length exponent ν_T^{FS} of order

$$\nu_T^{FS} = \nu_{loc} + \kappa_T = 1 + \kappa_T \simeq 1.25 \tag{36}$$

In another traveling/non-traveling phase transition studied in Ref [30] (see the summary in Appendix C), it has been obtained that the finite-size scaling exponent ν_{FS} is determined by the relaxation rate towards the finite value in the non-traveling phase. We have thus studied the relaxation length towards the finite value in the delocalized phase. We find that our data for $\ln T_N$ are compatible with the form

$$\overline{\ln T_N(W < W_c)} \simeq -(W_c - W)^{-\kappa_T} a_N \tag{37}$$

where a_N is a random stationary process as a function of N. We find that its autocorrelation function is exponential

$$C(N) \simeq e^{-\frac{N}{\xi_{relax}(W)}} \tag{38}$$

and we measure that the relaxation length $\xi_{relax}(W)$ diverges with an exponent

$$\xi_{relax}(W) \propto \frac{1}{(W_c - W)^{\nu_{relax}}} \quad \text{with} \quad \nu_{relax} \simeq 1.21 \tag{39}$$

of the order of the exponent ν_T^{FS} of Eq. 36. We thus obtain that the critical properties are qualitatively similar to the critical properties described in Ref [30] (see the summary in Appendix C) : the traveling phase is characterized by a velocity that vanishes linearly, but the finite size scaling is governed by the relaxation length towards the asymptotic finite value of the non-traveling phase. Exactly at criticality, we thus expects the following stretched exponential decay of the typical transmission

$$\overline{\ln T_N(W_c)} \simeq -N^{\rho_T} \tag{40}$$

where the exponent ρ_T is related to the other exponents by (see the scaling relations of Eqs C9 and C11 in Appendix C)

$$\rho_T = \frac{\kappa_T}{\nu_T^{FS}} = 1 - \frac{1}{\nu_T^{FS}} \tag{41}$$

From our previous estimate of the exponent $\kappa_T \simeq 0.25$, this would correspond to the numerical value

$$\rho_T = \frac{\kappa_T}{1 + \kappa_T} \simeq 0.2 \tag{42}$$

We have not been able to measure this stretched exponential behavior exactly at criticality from our data, because a precise measure of the exponent ρ_T would require to be exactly at the critical point.
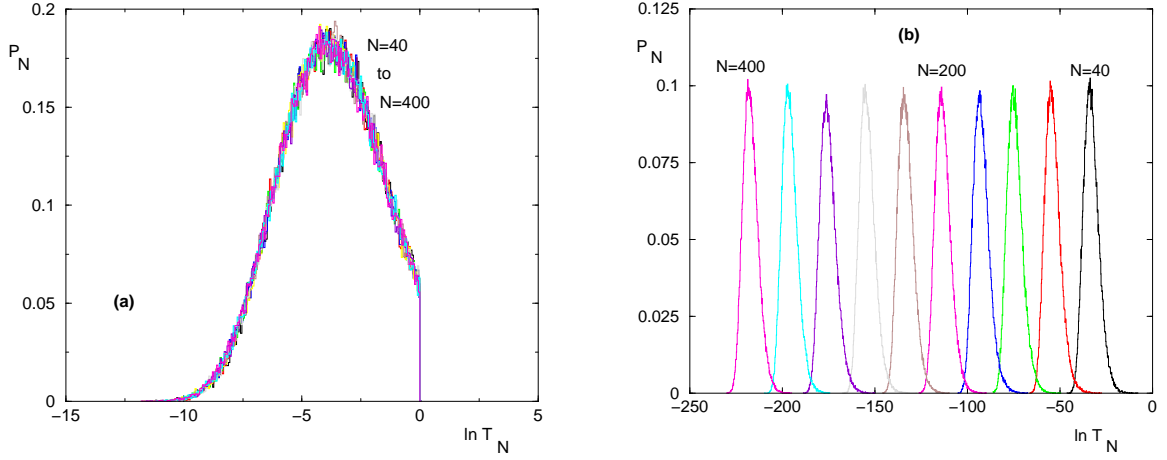
FIG. 4: Evolution with N of the probability distribution $P_N(\ln T_N)$ of the logarithm of Landauer transmission : (a) In the delocalized phase (here $W = 10$), the probability distribution $P_N(\ln T_N)$ does not move with N, and vanishes with a discontinuity at the boundary $\ln T_N = 0$. (b) In the localized phase (here $W = 25$), the probability distribution $P_N(\ln T_N)$ moves with N as a traveling wave of fixed shape.

5. Distribution of the logarithm of the transmission

Up to now, we have only discussed the behavior of the typical transmission of Eq. 29 as a function of N and W. We now turn to the probability distribution of the logarithm of the transmission around its averaged value, i.e. we consider the distribution of the relative variable

$$u \equiv \ln T_N - \overline{\ln T_N} \qquad (43)$$

We find that as $N \to \infty$, this variable remains finite not only in the delocalized phase where $\overline{\ln T_\infty}$ is finite, but also in the localized phase where $\overline{\ln T_N}$ decays linearly in N (Eq. 30). This means that in the localized phase, the probability distributions $P_N(\ln T_N)$ actually propagates as a traveling wave with a fixed shape around its moving center $\overline{\ln T_N}$ as shown on Fig. 4 (b). This phenomenon has already been seen for random scattering models on the Bethe lattice (see Fig. 8b of Ref. [20]). This is in contrast to the broadening with L observed in low dimensions $d = 1, 2, 3$ (see Eq. 2) : the Cayley tree thus corresponds to $\omega_{Cayley} = 0$ in Eq. 2.
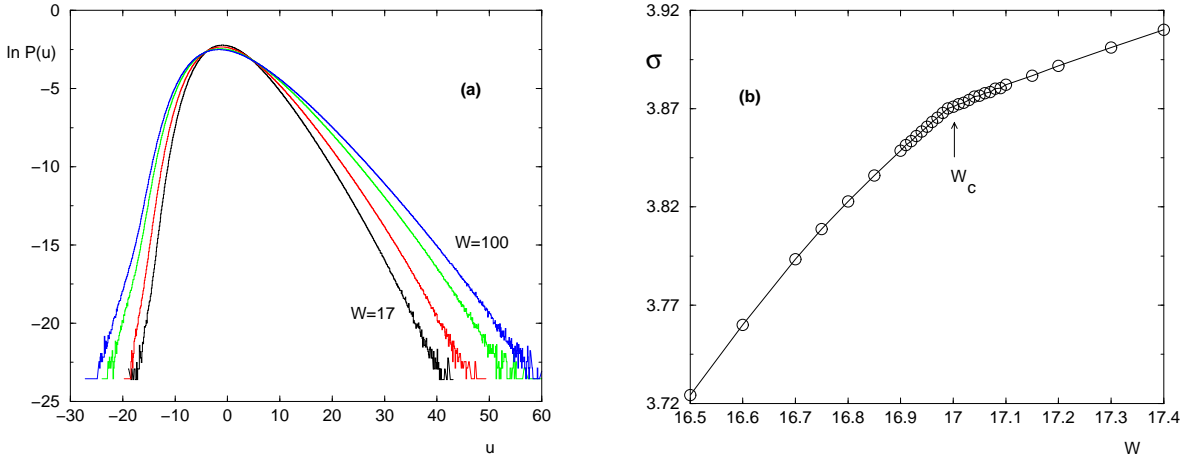

FIG. 5: (a) Logarithm of the probability distribution $P(u)$ of $u = \ln T_N - \overline{\ln T_N}$ as W varies in the localized phase for various disorder strengths $W = 17, 25, 50, 100$: the exponential decay as $e^{-\beta u}$ corresponds to slopes of order $\beta(W = 17) \simeq 0.48$, $\beta(W = 25) \simeq 0.43$, $\beta(W = 50) \simeq 0.35$, $\beta(W = 100) \simeq 0.33$. (b) Width $\sigma = (\overline{u^2})^{1/2}$ of the probability distribution of $u = \ln T_N - \overline{\ln T_N}$ as a function of W : it remains finite both in the localized phase and in the delocalized phase, but it presents a cusp singularity at criticality.

The fact that the shape is fixed can be used numerically to measure more precisely the tails of this probability

distribution by accumulating data over iterations : we show on Fig. 5 (a) the histograms of u obtained by this procedure for various disorder strength W. An essential property of this distribution is the right exponential tail

$$P_W(u) \underset{u \to +\infty}{\simeq} e^{-\beta(W)u} \tag{44}$$

In terms of the rescaled transmission $t = T_N/T_N^{typ} = e^u$ (see Eq. 43), this corresponds to the power-law decay

$$P(t = T_N/T_N^{typ}) \underset{t \to +\infty}{\simeq} \frac{1}{t^{1+\beta(W)}} \tag{45}$$

We find that the selected exponent $\beta_{selec}(W)$ slightly grows as the disorder strength W decreases, from a value of order $\beta(W = 100) \simeq 0.33$ for the strong disorder $W = 100$ towards a value of order $\beta(W = 17) \simeq 0.48$ near criticality (see Figure 5 a). The velocity of the traveling wave propagation of the whole distribution is actually determined by this power-law tail, as explained in detail in Appendix A. In particular, the critical value $\beta(W \to W_c) = 1/2$ has been predicted in [9] (see Eq. A33 in Appendix A). An important consequence of the power-law tail of Eq. 45 with $\beta(W) \leq 1/2$ is that all integer moments $\overline{T_N^n}$ of the Landauer transmission will be governed by rare events.

Finally, we show on Fig. 5 (b) the width of the probability distribution of $\ln T_N$ as a function of W : it remains finite both in the localized phase and in the delocalized phase, but it presents a cusp singularity at criticality because in the delocalized phase, the distribution presents a singularity at finite distance from the typical value, as is clearly visible on Fig. 4 (a) : the transmission is bounded by $T \leq 1$, i.e. the histogram of $\ln T_N$ presents a discontinuity at $\ln T_N = 0$.

III.   STATISTICS OF EIGENSTATES

The Landauer transmission studied in the previous section is of course the most appropriate observable to characterize the transport properties and to find the transition between the conducting/non-conducting phases. However, one expects that these transmission properties that emerge when the disordered sample is linked to incoming and outgoing wires are related to the nature of eigenstates of the disordered sample in the absence of these external wires (see Fig. 6) To determine whether a normalized eigenstate

$$\sum_x |\psi(x)|^2 = 1 \tag{46}$$

is localized or delocalized, the usual parameters are the Inverse Participation Ratios (I.P.R.)

$$I_q \equiv \sum_x |\psi(x)|^{2q} \tag{47}$$

of arbitrary power q. Another important quantity to characterize the spatial extent of an eigenstate is its entropy

$$S \equiv -\sum_x |\psi(x)|^2 \ln |\psi(x)|^2 \tag{48}$$

The normalization condition yields the identity $I_{q=1} = 1$, and the entropy corresponds to

$$S = -\partial_q I_q|_{q=1} = -\partial_q \ln I_q|_{q=1} \tag{49}$$

On an hypercubic lattice of size L in dimension d, containing $\mathcal{N}_L = L^d$ sites, the delocalized phase is characterized by the following typical behaviors

$$\overline{\ln I_q} \sim -d(q-1)\ln L = -(q-1)\ln \mathcal{N}_L \tag{50}$$

and

$$\overline{S} \sim d\ln L = \ln \mathcal{N}_L \tag{51}$$

These scalings are the same for pure homogeneous eigenfunctions with $|\psi(x)| = 1/L^d$ for all sites $x \in L^d$. At criticality, the scalings of the I.P.R. involve a whole series of non-trivial exponents and the wave function is said to be multifractal (see the review [7]). Finally in the localized phase, the I.P.R. and the entropy are finite.

In the present section, we discuss the statistical properties of these I.P.R. and entropy for zero-energy eigenstates for the Cayley tree of Fig. 6 as a function of the number N of tree generations and of the disorder strength W.
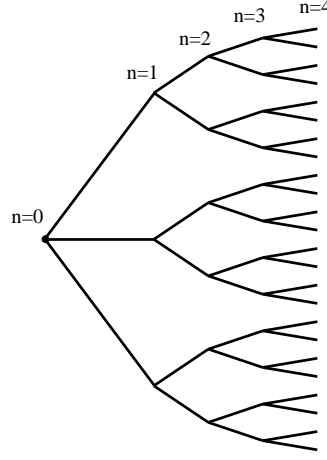
FIG. 6: Cayley tree with branching ratio $K = 2$ where each interior site has $K + 1 = 3$ neighbors. On the figure the tree ends at generation $2N = 4$.

A. Reminder on the Miller-Derrida framework to construct eigenstates

We refer to [17] where it is explained how eigenstates of finite trees can be constructed and how the density of states can be obtained. Note that on a tree, boundary sites dominate so that one needs a substraction procedure to obtain the appropriate bulk density of states. In the following, we are not interested into the density of states, which does not contain any information on the localized/delocalized nature of the spectrum. We wish to study instead the spatial properties of eigenstates of zero-energy $E = 0$ (center of the band). The Schrödinger equation 9 yields as before the recursion of Eq. 14 for the Riccati variables defined in Eq. 11. The difference with the scattering case is now in the boundary conditions

$$R(2N, j) = -\epsilon(2N, j) \tag{52}$$

that replace Eq. 13. As a consequence, the Riccati variables are now real (and not complex). The energy $E = 0$ will indeed be an eigenstate only if the Schrödinger equation is also satisfied at the center of the finite tree at the center site

$$0 = \epsilon(0) + \sum_{m=1}^{K+1} \frac{1}{R(des_m(0))} \tag{53}$$

Since the on-site energy $\epsilon(0)$ is a random variable drawn with some distribution, we may consider that we choose $\epsilon(0)$ to satisfy Eq. 53 to obtain a typical eigenstate of zero energy and to study its spatial properties. Let us first describe zero-energy eigenstate in the pure case to stress the peculiarities of the tree geometry.

B. Structure of zero-energy eigenstate on the pure tree

In the pure case where all on-site energies vanish $\epsilon(n, j) = 0$, the zero-energy eigenstate with radial symmetry reads

$$\psi_{2n-1} = 0 \tag{54}$$

$$\psi_{2n} = \psi_0 \left(-\frac{1}{K}\right)^n \tag{55}$$

where the root amplitude ψ_0 is determined by the normalization condition

$$
\begin{aligned}
1 &= \sum_x |\psi(x)|^2 = |\psi_0|^2 + (K+1)K|\psi_2|^2 + (K+1)K^3|\psi_4|^2 + ... + (K+1)K^{2N-1}|\psi_{2N}|^2 \\
&= |\psi_0|^2 \left[1 + \frac{K+1}{K}N\right]
\end{aligned}
\tag{56}
$$

This state is the analog of the scattering state described in section II B. In particular, one sees again an exponential decay of the wavefunction in this delocalized case which is very peculiar to the tree geometry : in the normalization condition of Eq. 56, this exponential decay is exactly compensated by the exponential growth of the number of sites at generation $2n$, so that all generations $2n = 2, 4, ..2N$ carry exactly the same weight in the normalization condition, and the root weight $|\psi_0|^2$ vanishes as $1/N$ in the thermodynamic limit, where $(2N)$ is the number of generations of the tree.

For this state, the usual Inverse Participation Ratio of Eq. 47 for $q = 2$ reads

$$I_2^{pur}(2N) \quad = \sum_x |\psi(x)|^4 = |\psi_0|^4 + (K+1)K|\psi_2|^4 + (K+1)K^3|\psi_4|^4 + ... + (K+1)K^{2N-1}|\psi_{2N}|^4 \tag{57}$$

$$= |\psi_0|^4 \left[1 + \frac{K+1}{K^3} \frac{1 - \left(\frac{1}{K^2}\right)^N}{1 - \frac{1}{K^2}} \right] \tag{58}$$

More generally for $q > 1$, one obtains the following decay with the number of generations

$$I_q^{pur}(2N) \underset{N\to\infty}{\propto} |\psi_0|^{2q} \sim \frac{1}{N^q} \quad \text{for} \quad q > 1 \tag{59}$$

In terms of the total number of sites

$$\mathcal{N}(2N) \quad = 1 + (K+1) \sum_{n=1}^{2N-1} K^n = 1 + (K+1)\frac{K^{2N}-1}{K-1} = \frac{K^{2N}(K+1) - 2}{K-1} \tag{60}$$

this corresponds to

$$\ln I_q^{pur}(2N) \underset{N\to\infty}{\propto} -q \ln N \underset{N\to\infty}{\propto} -q \ln(\ln \mathcal{N}(2N)) \quad \text{for} \quad q > 1 \tag{61}$$

This behavior is thus very anomalous with respect to the corresponding decay as $(-(q-1)\ln \mathcal{N}_L)$ for the I.P.P. of pure states in finite dimension d (see Eq. 50).

Moreover, since the eigenfunction normalization yields the idendity $I_{q=1} = 1$, one sees that there exists some discontinuity as $q \to 1$. In particular, the entropy of Eq. 48 which can usually be computed as the derivative of Eq. 49 should be computed directly here, and one obtains

$$S^{pur}(2N) \quad = -|\psi(0)|^2 \ln |\psi(0)|^2 - (K+1)K|\psi(2)|^2 \ln |\psi(2)|^2 - ... - (K+1)K^{2N-1}|\psi(2N)|^2 \ln |\psi(2N)|^2 \tag{62}$$

$$= |\psi(0)|^2 \left[-\left(1 + \frac{K+1}{K}N\right) \ln |\psi(0)|^2 + \frac{K+1}{K}N(N+1) \ln K \right] \tag{63}$$

Using Eq 56, one obtains the following behavior for large N

$$S^{pur}(2N) \quad = \ln\left(1 + \frac{K+1}{K}N\right) + \frac{\frac{K+1}{K}N(N+1)\ln K}{\left(1 + \frac{K+1}{K}N\right)} \underset{N\to\infty}{\simeq} N \ln K \tag{64}$$

In terms of the total number of sites of Eq. 60, the entropy is proportional to the logarithm of the number of sites

$$S^{pur}(2N) \underset{N\to\infty}{\simeq} N \ln K \underset{N\to\infty}{\simeq} \frac{1}{2} \ln \mathcal{N}(2N) \tag{65}$$

that should be compared with the growth as $\ln \mathcal{N}(2N)$ for pure eigenstates in dimension d (see Eq. 51).

In conclusion, the tree geometry induces very anomalous scalings in $(\ln \ln \mathcal{N})$ for the logarithm of I.P.R. of pure states (see Eq. 61) with respect to the case of finite dimension d, whereas the entropy is well behaved in $(\ln \mathcal{N})$ (see Eq. 65). In the disordered case, we expect to observe similar behaviors, whereas the I.P.R. and the entropy will remain finite in the localized phase.

C. Recursion relation for Inverse Participation Ratios (I.P.R.)

To compute the Inverse Participation Ratio I_q (Eq. 47) via recursion, one needs to introduce besides the Riccati variable of Eq. 11 the auxiliary variables defined by

$$C^{(q)}(n, j) = |\frac{\psi(n, j)}{\psi(anc(n, j))}|^{2q} + \sum_l |\frac{\psi(l)}{\psi(anc(n, j))}|^{2q} \tag{66}$$

where the sum is over all sites l that are descendants of the site (n, j) of the tree. These variables satisfy the following recurrence inside the tree $1 \leq n \leq 2N - 1$

$$C^{(q)}(n, j) = \left(\frac{1}{R^2(n, j)} \right)^q \left[1 + \sum_{m=1}^{K} C^{(q)}(des_m(n, j)) \right] \tag{67}$$

and the initial conditions at the boundaries

$$C^{(q)}(2N, j) = \left(\frac{1}{R^2(2N, j)} \right)^q \tag{68}$$

At the central root, on needs to impose the normalization

$$1 = \sum_x |\psi(x)|^2 = |\psi(0)|^2 \left[1 + \sum_{m=1}^{K+1} C^{(1)}(1, m) \right] \tag{69}$$

that determines the weight $|\psi(0)|^2$ of the root in terms of the variables $C^{(1)}$ of the branches.

To compute the inverse participation ratio of parameter q of Eq. 47, one needs the variables $C^{(q)}$ together with the variables $C^{(1)}$

$$I_q = \sum_x |\psi(x)|^{2q} = |\psi(0)|^{2q} \left[1 + \sum_{m=1}^{K+1} C^{(q)}(1, m) \right] = \frac{\left[1 + \sum_{m=1}^{K+1} C^{(q)}(1, m) \right]}{\left[1 + \sum_{m=1}^{K+1} C^{(1)}(1, m) \right]^q} \tag{70}$$

D. Recursion for the entropy

To compute recursively the entropy of Eq. 48, one needs similarly to introduce the auxiliary variable

$$\sigma(n, j) = - \sum_l \frac{|\psi_l|^2}{\sum_{l'} |\psi_{l'}|^2} \ln \frac{|\psi_l|^2}{\sum_{l'} |\psi_{l'}|^2} \tag{71}$$

where the sum over l denotes the sum over the site (n, j) and all its descendants : $\sigma(n, j)$ thus represents the entropy for the branch containing (n, j) and its descendants.

The initial conditions at the boundaries are simply

$$\sigma(2N, j) = 0 \tag{72}$$

and the recursion inside the tree $1 \leq n \leq 2N - 1$ can be written as

$$\sigma(n, j) = \frac{\sum_{m=1}^{K} C^{(1)}(des_m(n, j)) \sigma(des_m(n, j))}{1 + \sum_{m=1}^{K} C^{(1)}(des_m(n, j))} + S_{mix} \tag{73}$$

where the first term represents the weighted contribution of the branches entropies and where the second term represents the mixing entropy

$$S_{mix} = -p_0 \ln p_0 - \sum_{m'=1}^{K} p_{m'} \ln p_{m'} \tag{74}$$

with the weights

$$p_0 = \frac{1}{(1 + \sum_{m=1}^{K} C^{(1)}(des_m(n, j)))} \tag{75}$$

$$p_{m'} = \frac{C^{(1)}(des_{m'}(n, j)))}{(1 + \sum_{m=1}^{K} C^{(1)}(des_m(n, j)))} \tag{76}$$

$$\tag{77}$$

normalized to $p_0 + \sum_{m'=1}^{K} p_{m'} = 1$. At the central site of the tree, one uses the same formula but with $(K + 1)$ branches instead of K branches.

E. Numerical results on the statistics of eigenstates

1. Numerical pool method

To study the statistical properties of eigenstates, we have used again the pool method explained in II C 1. The only difference is that for the transmission, we have followed the recursions for the complex Riccati variables, whereas here we follow the recursions for the real Riccati variable R and for the auxiliary variables $C^{(1)}$, $C^{(2)}$ and σ described above.

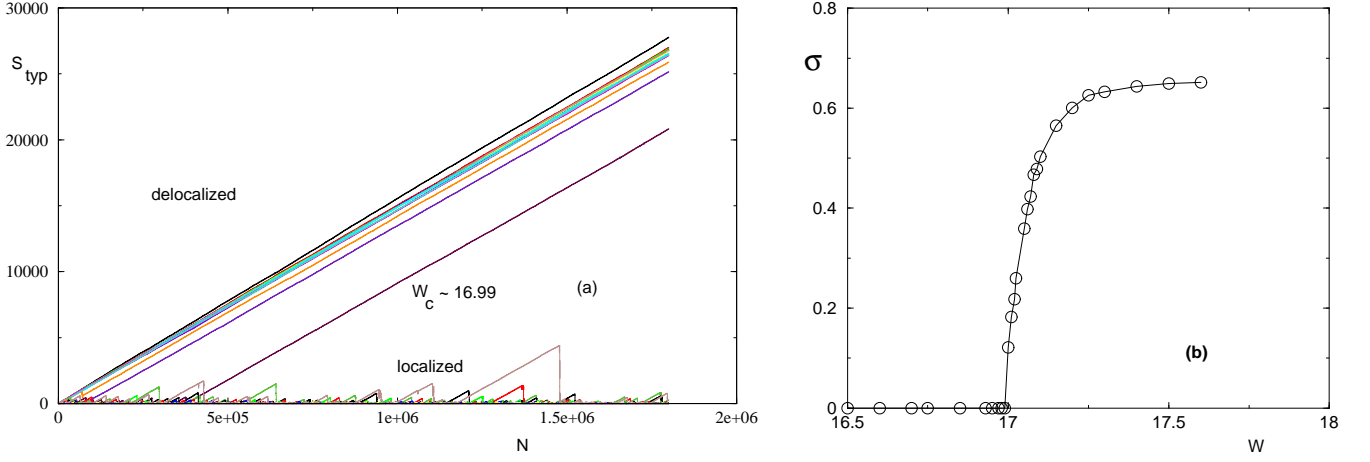### 2. Statistics of the entropy of an eigenstate

FIG. 7: Statistics of the entropy $S(N) \equiv -\sum_x |\psi(x)|^2 \ln |\psi(x)|^2$ of a normalized zero-energy eigenstate : (a) Evolution of the typical entropy $S_{typ}(N) \equiv e^{\overline{\ln S(N)}}$ with the number N of generations : it grows linearly in N in the delocalized phase, whereas it remains finite in the localized phase. (b) Asymptotic width $\sigma = (\overline{v^2})^{1/2}$ of the relative variable $v = \ln S - \overline{\ln S}$ as a function of the disorder strength W : the width converges to 0 (as $1/N$) in the delocalized phase, whereas it is finite in the localized phase

We first consider how the eigenstate entropy defined in Eq. 48 evolves with the number N of generations. As shown on Fig. 7 (a), the typical value grows linearly in N in the delocalized phase

$$S_{typ}(N, W < W_c) \equiv e^{\overline{\ln S(N)}} \underset{N \to \infty}{\simeq} aN \tag{78}$$

where the factor a varies smoothly with W and does not vanish continuously near the critical point. In this delocalized phase, we moreover find that the width of the relative variable $v = \ln S_N - \overline{\ln S_N}$ decays to zero as $N \to \infty$

$$\left[\overline{(\ln S_N - \overline{\ln S_N})^2} \right]^{1/2}_{W < W_c} \underset{N \to \infty}{\simeq} \frac{1}{N} \tag{79}$$

In the localized phase on the contrary, the typical value and the width of the relative variable $v = \ln S_N - \overline{\ln S_N}$ remain finite as $N \to +\infty$ (see Fig. 7 (a) and (b)).

As shown on Fig. 8, we find that the typical entropy of an infinite tree of the localized phase diverges with the following power law near criticality

$$S_{typ} \equiv e^{\overline{\ln S(N=+\infty)}} \underset{W \to W_c^+}{\simeq} \frac{1}{(W - W_c)^{\nu_S}} \quad \text{with} \quad \nu_S \simeq 1.5 \tag{80}$$

The entropy measures the size of the region where the weight $|\psi(x)|^2$ is concentrated, whereas the localization length $\xi_{loc} \sim 1/(W - W_c)^{\nu_{loc}=1}$ describes the far exponential decay of the transmission T (Eq. 30). We thus conclude that
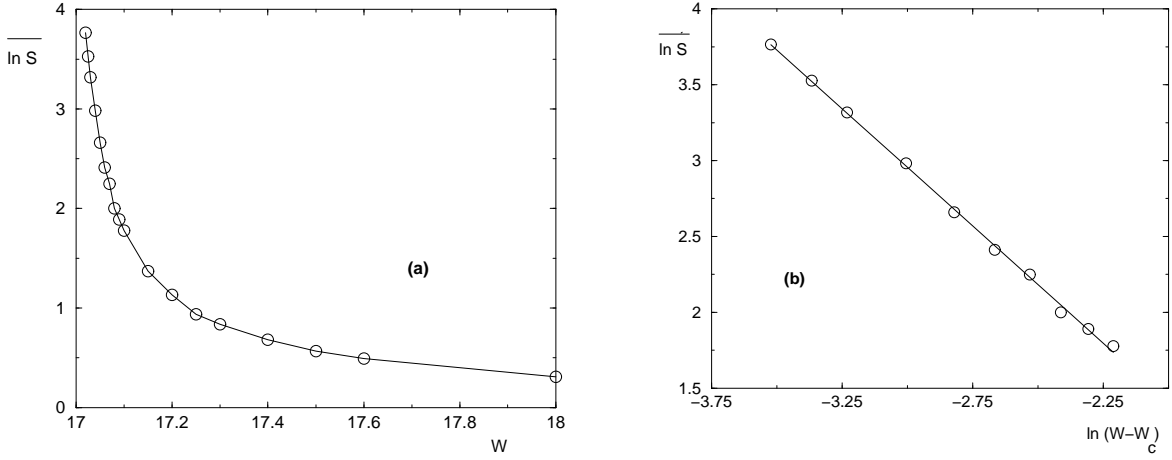
FIG. 8: Critical behavior of the typical entropy $S_{typ}(N = \infty) = e^{\overline{\ln S(N=\infty)}}$ in the localized phase (a) $\ln S_{typ}(N = \infty) = \overline{\ln S(N = \infty)}$ as a function of the disorder strength W near the critical point. (b) same data as a function of $\ln(W - W_c)$ to measure the exponent of the power law of Eq. 80 : the slope is of order $\nu_S \simeq 1.5$.

in the localized phase, besides the localization length $\xi_{loc} \sim 1/(W - W_c)^{\nu_{loc}=1}$ known since [10], there exists a larger diverging length scale

$$\xi_S(W > W_c) \underset{W \to W_c^+}{\propto} \frac{1}{(W - W_c)^{\nu_s \sim 1.5}} \tag{81}$$

that characterizes the size where the weight $|\psi(x)|^2$ is concentrated.

3. Statistics of the root weight $|\psi_N(0)|^2$ and of the I.P.R. I_2

As explained above, the root weight $|\psi_N(0)|^2$ and of the I.P.R. I_2 are determined by the auxiliary variables $C^{(q)}$ introduced in Eq. 66. We thus expect that the localized and delocalized phases correspond to the following behaviors for the auxiliary variables $C^{(q)}$

(i) in the localized phase, the auxiliary variables $C^{(q)}$ will remain finite random variables as the number of generations diverge $N \to \infty$. Then the root weight $|\psi_N(0)|^2$ and the I.P.R. I_q remain finite as $N \to \infty$.

(ii) in the delocalized phase, the auxiliary variables $C^{(q)}$ will instead grow exponentially with the number N of generations with some Lyapunov exponents $\lambda_q > 0$ defined by

$$\overline{\ln C^{(q)}} \underset{N \to \infty}{\simeq} \lambda_q N \tag{82}$$

The corresponding typical behaviors of the root weight and of the I.P.R. then reads

$$\overline{\ln |\psi_N(0)|^2} \underset{N \to \infty}{\simeq} -\lambda_1 N \tag{83}$$

and

$$\overline{\ln I_q} \underset{N \to \infty}{\simeq} -(q\lambda_1 - \lambda_q)N \tag{84}$$

We find numerically that the probability distributions of auxiliary variables $(\ln C^q)$ move as traveling waves of velocity λ_q (see Eq. 82) with fixed shape (see Figure 12 of Appendix B where the fixed shape is shown for $q = 1$ and $q = 2$). We explain in Appendix B how the Lyapunov exponents λ_q can be determined via a tail analysis that yields the identity (see Eq. B13)

$$\lambda_q = q\lambda_1 \tag{85}$$

so that the logarithm of the I.P.R. I_q decays slower than linearly in N, because the coefficient in Eq. 84 exactly vanishes. Physically, one could expect the decay to be of order $(\ln N)$ as in Eq. 61 concerning pure states on the

Cayley tree, but we have not been able to measure the behavior of the I.P.R., because within the pool method that we use, it turns out that the pool-dependent critical point is not the same for the variables $C^{(1)}$ and for $C^{(2)}$ (see more details in section B 3), so that it does not seem easy with the pool method to extract reliable results concerning I_2.

In the remaining of this section, we thus focus on the statistical properties of the root weight $|\psi(0)|^2$ that is determined by the auxiliary variable $C^{(1)}$ via Eq. 69. The fact that the pool-dependent critical point for $C^{(1)}$ is the same as the critical point found for the Landauer transmission can be understood from the tail analysis of the Appendices A and B that involve exactly the same integral kernel.
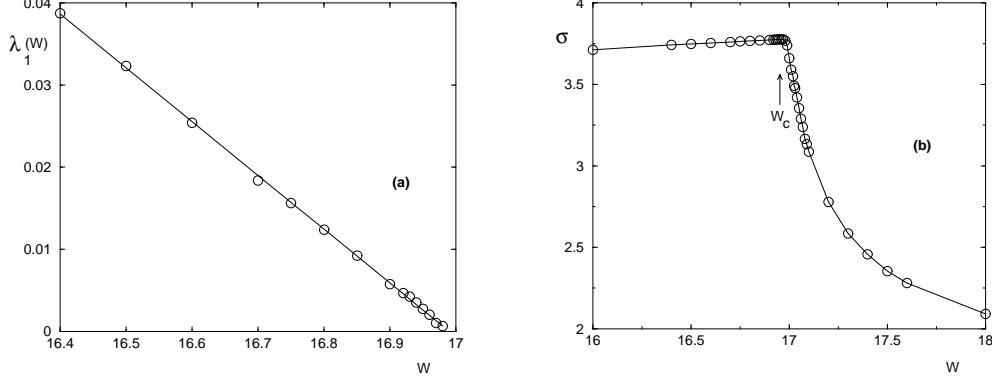

FIG. 9: (a) In the delocalized phase, the logarithm of the root weight decays linearly $\overline{\ln |\psi_N(0)|^2} \sim -\lambda_1(W)N$: the figure shows that the slope $\lambda_1(W)$ vanishes linearly $\lambda_1(W) \sim (W_c^{pool} - W)$ (see Eq. 86 with $\nu_{loc} = 1$). (b) Width $\sigma = (\overline{z^2})^{1/2}$ of the relative variable $z = \ln |\psi_N(0)|^2 - \overline{\ln |\psi_N(0)|^2}$ in the limit $N \to +\infty$ as a function of the disorder strength W : it remains finite both in the localized and delocalized phase, but it presents a cusp at the critical point W_c.

In the delocalized phase, the root weight $|\psi_N(0)|^2$ presents the typical decay of Eq. 83. We show on Fig. 9 (a) that the corresponding Lyapunov exponent $\lambda_1(W)$ vanishes linearly in the critical region

$$\lambda_1(W) \underset{W \to W_c^-}{\simeq} (W_c - W) \qquad (86)$$

i.e. we find the same exponent $\nu_{loc} = 1$ as for the divergence of the correlation length of the localized phase (see Eq. 32). This can be understood from the tail analysis presented in the Appendices A and B.

We find that the width of the relative variable $z = \ln |\psi_N(0)|^2 - \overline{\ln |\psi_N(0)|^2}$ remains finite in the limit $N \to +\infty$ both in the localized phase and in the delocalized phase : its behavior as a function of the disorder strength W presents a cusp at W_c as shown on Fig. 9 (b).
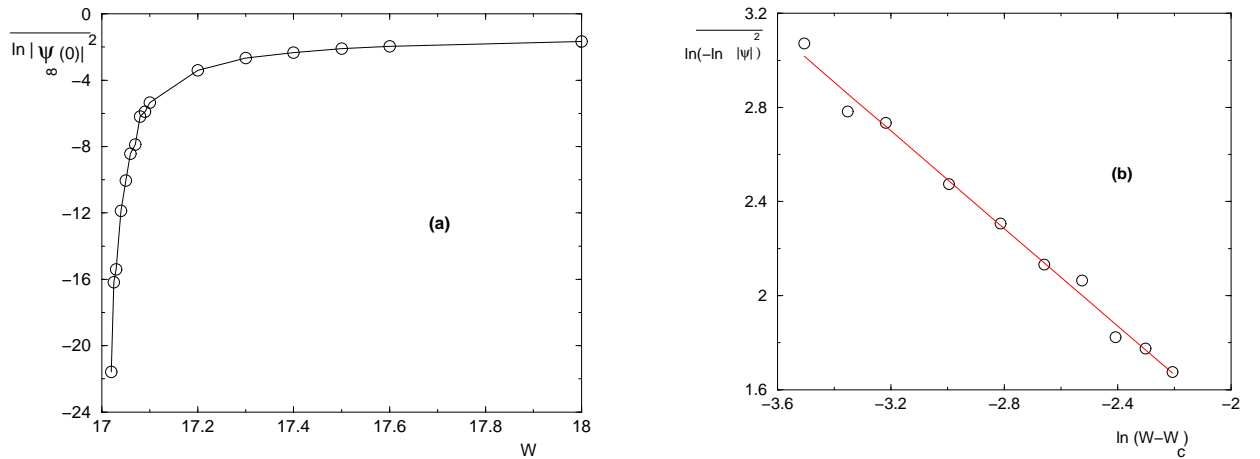

FIG. 10: Critical behavior of the root weight $|\psi_\infty(0)|^2$ of an infinite tree in the localized phase : (a) $\overline{\ln |\psi_\infty(0)|^2}$ as a function of the disorder strength W (b) $\ln(-\overline{\ln |\psi_\infty(0)|^2})$ as a function of $\ln(W - W_c)$ to measure the exponent of the essential singularity of Eq. 87 : we measure asymptotically a slope of order $\kappa_0 \sim 1$.

In the localized phase, the root weight remains finite as $N \to \infty$. As show on Fig. 10, we measure the following essential singularity

$$\overline{\ln \psi_\infty(0)} \underset{W \to W_c^+}{\simeq} -\frac{1}{(W - W_c)^{\kappa_0}} \quad \text{with} \quad \kappa_0 \simeq 1 \tag{87}$$

As in section II C 4, we now discuss the finite-size scaling in the critical region. If there exists some finite-size scaling in the critical region for the typical root weight, the matching of our results in the delocalized phase (see Eq. 83 and 86) and in the localized phase (Eq. 87) requires a finite-size correlation length exponent ν_0^{FS} of order

$$\nu_0^{FS} = 1 + \kappa_0 \simeq 2. \tag{88}$$

We have performed the analysis described in section II C 4 and we measure that the relaxation length $\xi_{relax}(W)$ towards the finite value of Eq. 87 diverges with an exponent

$$\xi_{relax}(W) \propto \frac{1}{(W - W_c)^{\nu_{relax}}} \quad \text{with} \quad \nu_{relax} \simeq 2. \tag{89}$$

of the order of the exponent ν_0^{FS} of Eq. 88. We thus obtain that the critical properties are again qualitatively similar to the critical properties described in Ref [30] (see the summary in Appendix C) : the traveling phase is characterized by a velocity that vanishes linearly, but the finite size scaling is governed by the relaxation length towards the asymptotic finite value of the non-traveling phase. Exactly at criticality, we thus expects the following stretched exponential decay of the typical transmission

$$\overline{\ln |\psi_N(0)|^2}|_{W=W_c} \simeq -N^{\rho_0} \tag{90}$$

where the exponent ρ_0 is related to the other exponents by (see the scaling relations of Eqs C9 and C11 in Appendix C)

$$\rho_0 = \frac{\kappa_0}{\nu_0^{FS}} = 1 - \frac{1}{\nu_0^{FS}} \tag{91}$$

From our previous estimate of the exponent $\kappa_0 \simeq 1.$, this corresponds to the numerical value

$$\rho_0 = \frac{\kappa_0}{1 + \kappa_0} \simeq 0.5 \tag{92}$$

Again, as explained after Eq. 42, we have not been able to measure this stretched exponential behavior exactly at criticality from our data, because a precise measure of the exponent ρ_0 would require to be exactly at the critical point.

IV. CONCLUSIONS AND PERSPECTIVES

In summary, for the Anderson model on the Bethe lattice, we have studied numerically the statistics of the Landauer transmission T_N and the statistics of eigenstates at the center of the band $E = 0$, as a function of the disorder strength W and the number N of generations. We have shown that both the localized phase and the delocalized phase are characterized by the traveling wave propagation of some probability distributions. In the text, we have presented detailed numerical results, and in Appendices A and B, we have explained how the velocities of the traveling waves are determined by the tails, via the properties of the integral kernel introduced in [9]. The Anderson transition then corresponds to a traveling/non-traveling critical point for these traveling waves, and the critical properties obtained are very similar to the traveling-wave phase transition studied in [30] : (i) the finite value of the non-traveling phase presents an essential singularity (ii) the relaxation length towards this essential singularity determines the finite-size scaling in the critical region (iii) the finite-size correlation length exponent ν_{FS} is different from the value $\nu_{loc} = 1$ that govern the vanishing of the velocity in the traveling-wave phase. We thus hope that in the future, these properties for Anderson localization on the Cayley tree will be better understood by extending the methods that have been developed recently for the class of the Fisher-KPP traveling waves (see [30, 43] and references therein).

How results obtained on the Bethe lattice are related to properties of Anderson localization in finite dimension d is of course a difficult question. During the history of localization, many values for the upper critical dimension have been proposed such as $d_c = 4, 6, 8, +\infty$. Even within the supersymmetric community, there seems to be different interpretations. Mirlin and Fyodorov [45] consider that the essential singularities that appear on the Bethe lattice,

are directly related to the exponential growth of the number of sites with the distance, and will become conventional power-law behaviors as soon as $d < \infty$, so that the upper critical dimension is actually $d_c = +\infty$. On the contrary, Efetov [15] argues that the results obtained for the Bethe lattice are relevant to Anderson transition in high dimension d when reinterpreted within the so-called 'effective medium approximation'. For the Landauer transmission, the upper critical dimension d_c can be defined as the dimension where the exponent $\omega(d)$ concerning the width of the sample-to-sample distribution in the localized phase (see Eq.2) vanishes $\omega(d_c) = 0$. This means that for $d \geq d_c$, the probability distribution would travel as a traveling wave in the whole localized phase. To determine whether $d_c = +\infty$ or $d_c < +\infty$, it would be thus interesting to understand whether the traveling wave propagation with a fixed shape is possible only on trees or whether it can also occur in sufficiently high dimension d.

In low dimensions, the probability distribution of the logarithm of the transmission is known to broaden with some exponent $\omega(d) > 0$ (see Eq. 2) in the localized phase, whereas the probability distribution of the logarithm of I.P.P. is known to shrink with the system size in the delocalized phase [46] (see also Fig. (4a) of [49] where the same phenomenon occurs for the directed polymer in $1 + 3$ dimensions). However traveling wave propagations of the probability distribution $P(\ln I_q)$ of Inverse Participation Ratios I_q have actually been found in finite dimensions but only *exactly at criticality*. This phenomenon has been first obtained for the power-law random band matrix model [47] and has been then observed for the Anderson model in dimensions $d = 3, 4$ [48] : the motions of the typical values $\overline{\ln I_q}$ with $(\ln L)$ determine the multifractal spectrum, whereas the reduced variables $y = I_q/I_q^{typ}$ keep fixed distributions presenting power-law tails with q-dependent exponents. We have actually observed the same behavior for the directed polymer in $1 + 3$ dimensions exactly at the localization/delocalization transition (see Fig. (3a) and (3b) of Ref. [49]). In all these cases, it would be thus very nice to better understand the relations between the tails of the distributions and the motions of the typical values, and to identify the wave equation that underlies these traveling waves.

Finally, our work raises once again the question whether Anderson transitions are characterized by several length scales that diverge with various ν exponents. Here for the Cayley tree, besides the exponent $\nu_{loc} = 1$ that has been predicted for a long time [10], we have found other diverging lengths with the following physical meanings. (i) in the localized phase, besides the exponent $\nu_{loc} = 1$ associated to the divergence of localization length $\xi_{loc} \sim 1/(W - W_c)^{\nu_{loc}=1}$ that describes the far exponential decay of the transmission T (Eq. 30), we have found that the critical behavior of the entropy is governed by another diverging length scale with $\nu_s \sim 1.5$ (Eq. 81) that characterizes the size where the weight $|\psi(x)|^2$ is concentrated. (ii) in the delocalized phase, we have found that the Landauer transmission reaches its asymptotic value after a length diverging as $\nu_T^{FS} \sim 1.25$ (Eq. 36) that governs the finite-size scaling of the transmission in the critical region. Even if the precision of numerically measured critical exponents can be always discussed, we feel nevertheless that our numerical results are not compatible with the existence of the single exponent $\nu_{loc} = 1$. Note that for the directed polymer on the Cayley tree, we have also found previously that the critical properties involve two exponents $\nu = 2$ and $\nu' = 1$ [50]. Whether there exists various exponents ν for Anderson model in finite dimension d has been debated for a long time. The majority of papers on Anderson localization seem in favor of a single ν (see the reviews [2–7]), but it seems to us that numerical papers actually study always the same type of observables. In particular, we have not been able to find numerical studies concerning the entropy of eigenstates. On the theoretical side, we are not aware of many theories in favor of various ν exponents, except (i) the supersymmetric studies of Refs [14, 15] that involve two different diverging length scales, called respectively the localization length and the phase coherence length. (ii) the pseudo-delocalization transition of the random hopping model in dimension $d = 1$, that is characterized by the two exactly known correlation lengths exponents $\nu = 1$ and $\nu = 2$ (see [51] and references therein), as in the other models described by the same strong disorder fixed point (see the review [52]). We feel that if localization models exhibit several ν exponents both on the Cayley tree which represents some mean-field $d = \infty$ limit and in some models in dimension $d = 1$, the possibility of various ν for Anderson transition in dimension $d = 3$ should be reconsidered by studying in detail the statistics of various observables.

APPENDIX A: TAIL ANALYSIS FOR THE TRAVELING WAVE OF THE LANDAUER TRANSMISSION IN THE LOCALIZED PHASE

In this Appendix, we translate the analysis of Ref. [9] concerning the distribution of the self-energy in the localized phase for the traveling-wave propagation of the Landauer transmission discussed in section II.

The recursion of Eq. 14 for the complex Riccati variable R_n reads more explicitly in terms of its real and imaginary parts $R_n = X_n - iY_n$ with $X_n \in]-\infty, +\infty[$ and $Y_n \in [0, +\infty[$.

$$X_n = -\epsilon_n - \sum_{m=1}^{K} \frac{X_{n-1}(m)}{X_{n-1}^2(m) + Y_{n-1}^2(m)} \tag{A1}$$

$$Y_n = \sum_{m=1}^{K} \frac{Y_{n-1}(m)}{X_{n-1}^2(m) + Y_{n-1}^2(m)} \tag{A2}$$

where the random on-site energies ϵ_n are drawn from the flat distribution of Eq. 4. The Landauer transmission of Eq. 26 then reads

$$T_n = 1 - \left| \frac{X_n + i(1 - Y_n)}{-X_n + i(1 + Y_n)} \right|^2 = \frac{4Y_n}{X_n^2 + (Y_n + 1)^2} \tag{A3}$$

In the delocalized phase, this recursion of Eq. A2 is difficult to analyze because one has to find the joint distribution of the two finite variables (X, Y) that remain stable upon iteration. In the localized phase however, the problem is simpler [9] as we now recall.

1. Linearized recursions in the localized phase

In the localized phase, if the imaginary part Y_n converge towards zero exponentially in n as

$$Y_n = e^{-vn} y_n \tag{A4}$$

where $v > 0$ and where y_n remains a finite random variable upon iteration, one has then to study the simpler recurrence for large n [9, 17]

$$X_n = -\epsilon_n - \sum_{m=1}^{K} \frac{1}{X_{n-1}(m)}$$

$$e^{-v} y_n = \sum_{m=1}^{K} \frac{y_{n-1}(m)}{X_{n-1}^2(m)} \tag{A5}$$

Note that the form of Eq. A4 corresponds to a traveling wave of velocity v for the variable $(\ln Y_n)$

$$\ln Y_n = -vn + \ln y_n \tag{A6}$$

The real part X_n satisfies now a closed recurrence independent of the Y_n, and its stable distribution $P^*(X)$ satisfies the closed equation

$$P^*(X) = \int d\epsilon p(\epsilon) \int dX_1 P^*(X_1) ... \int dX_m P^*(X_m) \delta \left[X + \epsilon + \sum_{m=1}^{K} \frac{1}{X_m} \right] \tag{A7}$$

An important property of this distribution is that it presents the power-law tail

$$P^*(X) \underset{X \to \pm\infty}{\simeq} \frac{KP^*(0)}{X^2} \tag{A8}$$

because whenever one of the K variables X_i on the right handside of Eq. A7 is close to 0, the variable X of the left-handside is large with $X \sim -1/X_i$.

The stable joint distribution $P^*(X, y)$ satisfies

$$P^*(X, y) = \int d\epsilon p(\epsilon) \int dX_1 dy_1 P^*(X_1, y_1) ... \int dX_m dy_m P^*(X_m, y_m) \delta \left[X + \epsilon + \sum_{m=1}^{K} \frac{1}{X_m} \right] \delta \left[y - \sum_{m=1}^{K} \frac{y_m}{e^{-v} X_m^2} \right] \tag{A9}$$

2.   Tail analysis

The idea of [9] is to look for the power-law tail in y that is compatible with the recursion equation, i.e. one assumes

$$P^*(X,y) \underset{y \to \infty}{\simeq} \frac{A(X)}{y^{1+\beta}} \tag{A10}$$

with some exponent $0 < \beta < 1$. Note that, in the traveling wave language of Eq. A6, this is equivalent to look for solutions with an exponential tail $e^{-\beta u}$ for the variable $u = \ln Y_n + nv = \ln y_n$. So this corresponds to the usual exponential tail analysis of fronts [28, 29], except for the following difference : in usual studies of propagation into unstable phases, it is the 'forward tail' that has an exponential decay and that determines the velocity, whereas in our present case, it is the 'backward tail' that determines the propagation.

In Laplace transform with respect to y, the power-law decay of Eq. A10 corresponds to the following singular expansion near the origin

$$\hat{P}^*(X;s) \equiv \int_0^{+\infty} dy e^{-sy} P^*(X,y) \quad = P^*(X) - \int_0^{+\infty} dy (1 - e^{-sy}) P^*(X,y) = P^*(X) - \int_0^{+\infty} \frac{dv}{s}(1 - e^{-v}) P^*(X, \frac{v}{s})$$

$$\underset{s \to 0}{\simeq} P^*(X) - s^\beta A(X) \int_0^{+\infty} dv \frac{(1 - e^{-v})}{v^{1+\beta}} \tag{A11}$$

Equation A9 becomes for the Laplace transform $\hat{P}^*(X;s)$

$$\hat{P}^*(X;s) = \int d\epsilon p(\epsilon) \int dX_1 \hat{P}^*(X_1, \frac{s}{\lambda X_1^2})... \int dX_m \hat{P}^*(X_m, \frac{s}{\lambda X_m^2}) \delta \left[X + \epsilon + \sum_{m=1}^K \frac{1}{X_m} \right] \tag{A12}$$

Using the expansion of Eq. A11, one obtains that the function $A(X)$ has to satisfy the eigenvalue equation

$$e^{-v\beta} A(X) = K \int \frac{dX_1}{(X_1^2)^\beta} Q(X + \frac{1}{X_1}) A(X_1) \tag{A13}$$

where the function $Q(u)$ represents the stationary distribution of the variable $u = -\epsilon - \sum_{m=2}^K \frac{1}{X_m}$

$$Q(u) = \int d\epsilon p(\epsilon) \int dX_2 P^*(X_2)... \int dX_m P^*(X_m) \delta \left[u + \epsilon + \sum_{m=2}^K \frac{1}{X_m} \right] \tag{A14}$$

(see Eqs 6.5 and 6.6 in [9]).

3.   Eigenvalue problem for an integral kernel

The tail analysis thus leads to the eigenvalue problem the integral kernel appearing in Eq. A13

$$\Lambda A(X) = K \int \frac{dX_1}{(X_1^2)^\beta} Q(X + \frac{1}{X_1}) A(X_1) \tag{A15}$$

For each β and W, the integral kernel is positive, and thus one expects some continuous analog of the Perron-Froebenius theorem : the iteration of the integral kernel will converge towards a positive eigenvector $A_0(X)$ that is associated to the maximal eigenvalue $\Lambda_0(\beta, W)$ of the kernel. For instance, for the special case $\beta = 0$, the solution is simply $A(X) = P^*(X)$ (see Eqs A7 and A14) and

$$\Lambda_0(\beta = 0, W) = K \tag{A16}$$

Except for this case $\beta = 0$, we are not aware of any explicit solution for the eigenvalue $\Lambda_0(\beta, W)$ (even for the simpler case where the distribution of the on-site energies $p(\epsilon)$ is a Cauchy law and where the distributions $P(X)$ and $Q(u)$ are also Cauchy laws [9, 17]). With Eqs A13 and A15, one concludes that at fixed W, each mode β is associated to the velocity $v(\beta, W)$ (Eq. A4)

$$v(\beta, W) = -\frac{1}{\beta} \ln \Lambda_0(\beta, W) \tag{A17}$$

4. Selection of the tail exponent and of the velocity of the traveling wave

The selection of the tail exponent β of Eq. A10 and of the corresponding velocity $v(\beta)$ of Eq A4 usually depend on the form of the initial condition [26, 28, 29]. In our present case, the initial condition is completely localized (see Eq. 13)

$$P_{ini}(Y) = \delta(Y - 1) \tag{A18}$$

In this case, one expects that the solution that will be dynamically selected [26, 28, 29] corresponds to the tail exponent $\beta_{selec}(W)$ and to the velocity $v_{selec}(W) = v(\beta_{selec}(W), W)$ determined by the following extremization

$$0 = [\partial_\beta v(\beta, W)]_{\beta = \beta_{selec}(W)} = \left[\frac{1}{\beta^2} \ln \Lambda_0(\beta, W) - \frac{1}{\beta} \frac{\partial_\beta \Lambda_0(\beta, W)}{\Lambda_0(\beta, W)} \right]_{\beta = \beta_{selec}(w)} \tag{A19}$$

The critical point is then determined by the two conditions

$$v(\beta_c, W_c) = 0 \tag{A20}$$
$$\partial_{\beta_c} v(\beta_c, W_c) = 0 \tag{A21}$$

5. Example in the 'strong disorder approximation'

Since the general discussion is rather obscured by the absence of an explicit expression for the eigenvalue $\Lambda_0(\beta, W)$ of the kernel of Eq. A15, it is useful to consider the following strong disorder approximation (called 'upper limit' condition in [9]), where the recursion for the X_n in Eq. A5 is simply replaced by [9]

$$X_n \simeq \epsilon_n \tag{A22}$$

The argument is that in the limit of very large W, the distribution of X has also a width of order W, so that the neglected terms in Eq. A5 are of order K/W. Of course the approximation of Eq. A22 is not very well controlled, because it concerns random variables, and it suppresses important correlations between the variables (X, Y) of Eq. A5. Nevertheless, it is useful to consider it before returning to the true recursions of Eq. A5, because with Eq. A22, the eigenvalue $\Lambda_0(\beta, W)$ is replaced by simple expression [9] (see also section 7.2 of [17] where the approximation of independence between (X, Y) is considered for the Cauchy case)

$$\Lambda_0^{SD}(\beta, W) = K \int d\epsilon p(\epsilon) |\epsilon|^{-2\beta} \tag{A23}$$

The velocity then reads

$$v^{SD}(\beta, W) = -\frac{1}{\beta} \ln \left(K \int d\epsilon p(\epsilon) |\epsilon|^{-2\beta} \right) \tag{A24}$$

For the flat distribution $p(\epsilon)$ of random site energies (Eq. 4), one thus obtains

$$v^{SD}(\beta, W) = -\frac{1}{\beta} \ln \left(\frac{K}{1 - 2\beta} \left(\frac{2}{W} \right)^{2\beta} \right) = 2 \ln \frac{W}{2} - \frac{1}{\beta} \ln \left(\frac{K}{1 - 2\beta} \right) \tag{A25}$$

The function $v^{SD}(\beta)$ is defined on the interval $0 < \beta < 1/2$: it flows towards $(-\infty)$ in the limits $\beta \to 0$ and $\beta \to 1/2$ with the following behaviors

$$v^{SD}(\beta, W) \underset{\beta \to 0}{\simeq} -\frac{\ln K}{\beta} \tag{A26}$$

and

$$v^{SD}(\beta, W) \underset{\beta \to 1/2}{\simeq} -\frac{1}{\beta} \ln \frac{1}{1 - 2\beta} \tag{A27}$$

It has a single maximum at β_{selec}^{SD} given by the extremum condition of Eq. A19, so that β_{selec}^{SD} is actually independent of W. For $K = 2$, the selected exponent is of order $\beta_{selec}^{SD} \simeq 0.3133$ for any W. We note that is value is close to the value $\beta(W = 100) \simeq 0.33$ that we measure for the large disorder $W = 100$ (see Figure 5 a). In conclusion, this 'strong disorder approximation' allows to see explicitly how things work on a simple example, and seems to give a reasonable value of β_{selec} for very large W.

6. Argument in favor of $0 < \beta_{selec}(W) < 1/2$

We now return to the analysis of the full problem of Eq. A5. Here we should say that we do not agree with the discussion of [9] concerning the selection of the tail exponent β :

(i) in [9], the authors conclude that within the localized phase, $\beta_{selec}(W)$ decreases from unity and reaches $\beta_c = 1/2$ exactly at criticality (see the text between Eqs. 6.8 and 6.9 in [9]).

(ii) in our numerical results of section II we have found instead that the selected exponent $\beta_{selec}(W)$ is always smaller than $1/2$: it slightly grows as the disorder strength W decreases and has a value close to 0.5 near criticality (see Figure 5 a).
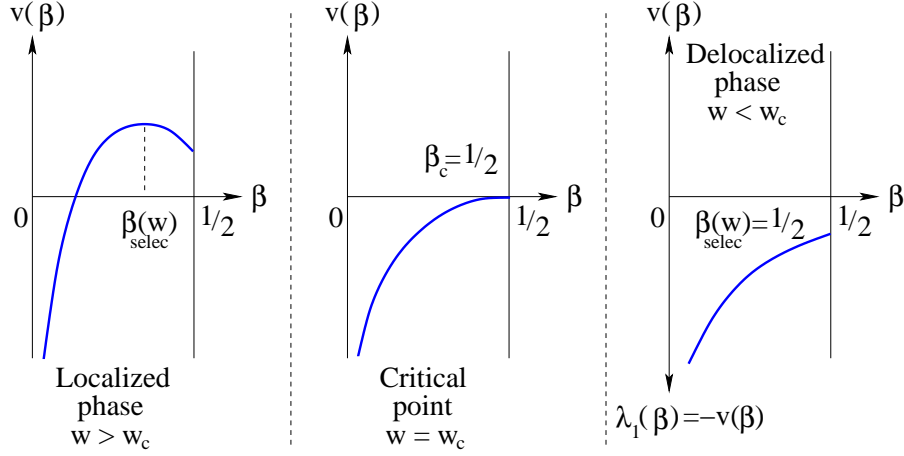

FIG. 11: Shape of the velocity $v(\beta, W)$ as a function of the tail exponent β for various disorder strength W : (i) in the localized phase $W > W_c$, the velocity is extremum at a W-dependent value $\beta_{selec}(W) < 1/2$ and it is positive $v_{selec} > 0$ (ii) at the critical point $W = W_c$, the velocity is extremum at $\beta_c = 1/2$ where it vanishes $v_c = 0$ (iii) in the delocalized phase, there exists another traveling-wave moving in the other direction of velocity $\lambda_1(\beta, W) = -v(\beta, W) > 0$: this velocity is extremum at $\beta = 1/2$ for any $W < W_c$ (see Appendix B for more details)

We propose the following argument to justify our finding $0 < \beta_{selec}(W) < 1/2$. We think that the tail analysis is actually well defined only on the interval $0 < \beta < 1/2$ for the following reasons. The eigenvalue Eq. A15 relates the behavior of $A(X)$ at $|X| \to \infty$ to the behavior of $A(X)$ near the origin $X \to 0$. For $X \to \infty$, the function $Q(X + \frac{1}{X_1})$ will be finite in the region where $(X + \frac{1}{X_1})$ is finite, i.e. the integration is dominated by the region $X_1 \sim -1/X$ and we obtain the power-law decay

$$A(X) \underset{|X| \to \infty}{\simeq} \frac{KA(0)}{\Lambda_0(\beta)|X|^{2-2\beta}} \tag{A28}$$

However the function $A(X)$ has to be integrable at $|X| \to \infty$ to obtain from Eq. A10 the probability of the variable y alone at large y

$$P^*(y) = \int_{-\infty}^{+\infty} dX P^*(X, y) \underset{y \to \infty}{\simeq} \frac{\int_{-\infty}^{+\infty} dX A(X)}{y^{1+\beta}} \tag{A29}$$

According to Eq. A28, the function $A(X)$ is integrable only for

$$0 < \beta < \frac{1}{2} \tag{A30}$$

i.e. we obtain that the tail analysis has a meaning only for $0 \le \beta < 1/2$. In the limit $\beta \to 0$, we expect from Eq. A16 the same behavior as in Eq. A26

$$v(\beta, W) \underset{\beta \to 0}{\simeq} -\frac{\ln K}{\beta} \tag{A31}$$

Exactly at $\beta = 1/2$, the authors of [9] have argued that

$$[\partial_\beta \Lambda_0(\beta, W)]_{\beta=1/2} = 0 \tag{A32}$$

for any W, as a consequence of the symmetry $\Lambda_0(\beta, W) = \Lambda_0(1-\beta, W)$ coming from the consideration of the adjoint kernel (see more details around Eqs. 6.7 and 6.8 in [9]). Here in contrast to [9], we think that the region $\beta > 1/2$ is not physical because of Eq. A28, but the condition of Eq. A32 is useful to understand why the critical point determined by Eqs A21 corresponds to the tail exponent [9]

$$\beta(W) \underset{W \to W_c^+}{\simeq} \beta_c = \frac{1}{2} \tag{A33}$$

To summarize the selection mechanism, the shape of the velocity $v(\beta, W)$ as a function of the tail exponent β in shown on Fig. 11 for various disorder strength W :

(i) in the localized phase $W > W_c$, the velocity derivative is negative at $\beta = 1/2$:

$$[\partial_\beta v(\beta, W > W_c)]_{\beta=1/2} = \left[\frac{1}{\beta^2} \ln \Lambda_0(\beta, W > W_c)\right]_{\beta=1/2} = -\left[\frac{1}{\beta} v(\beta, W > W_c)\right]_{\beta=1/2} < 0 \tag{A34}$$

The velocity is extremum at a W-dependent value $\beta_{selec}(W) < 1/2$ and the corresponding selected velocity is positive $v_{selec} > 0$.

(ii) at the critical point $W = W_c$, the velocity is extremum at $\beta_c = 1/2$ where it vanishes $v_c = 0$.

(iii) in the delocalized phase, the velocity derivative is positive at $\beta = 1/2$:

$$[\partial_\beta v(\beta, W < W_c)]_{\beta=1/2} = \left[\frac{1}{\beta^2} \ln \Lambda_0(\beta, W < W_c)\right]_{\beta=1/2} = -\left[\frac{1}{\beta} v(\beta, W < W_c)\right]_{\beta=1/2} > 0 \tag{A35}$$

We explain in Appendix B that in this delocalized phase, there exists another traveling-wave moving in the other direction with the velocity $\lambda_1(\beta, W) = -v(\beta, W) > 0$: this velocity $\lambda_1(\beta, W)$ is then extremum at $\beta = 1/2$ for any $W < W_c$ (see Appendix B for more details).

As a final remark, we believe that the solution exactly at W_c is not valid anymore because of Eq. A28, and that the appropriate treatment exactly at criticality should replace the finite velocity motion in vn assumed in Eq. A6 by the form

$$\ln Y_n = -(cst)n^\rho + \ln y_n \tag{A36}$$

where the anomalous exponent $0 < \rho < 1$ has been discussed in the text (see Eqs 35 and 42).

7. Conclusion

In conclusion, the analysis of [9] is thus very close to the traveling wave analysis of the directed polymer model [26]: the difference is that in the directed polymer, the variables X_n are random variables independent of the Y_n and the selected β_{selec} can be simply obtained from the non-integer moments of X (see the section 7.2 in [17]), whereas in the present localization model, the variables X_n and Y_n are correlated and one has thus to solve the eigenvalue problem for the integral kernel of Eq. A15. In the following Appendix, we explain how the same ideas can be used in the delocalized phase.

APPENDIX B: TAIL ANALYSIS FOR THE TRAVELING WAVES IN THE DELOCALIZED PHASE

As explained in section III, in the delocalized phase, we have considered the recurrence for the real Riccati variable X_n

$$X_n = -\epsilon_n - \sum_{m=1}^{K} \frac{1}{X_{n-1}(m)} \tag{B1}$$

together with the recurrences of Eqs 67 for the auxiliary variables $C^{(q)}$ introduced in Eq. 66.

1. Tail analysis leading to the same integral kernel as in Appendix A

To make more visible the similarities with the previous Appendix, it is convenient to perform the change of variables

$$D_n^{(q)} \equiv (X_n^2)^q C_n^{(q)} \tag{B2}$$

to obtain the following recursions for these variables

$$D_n^{(q)} = 1 + \sum_{m=1}^{K} \frac{D_{n-1}^{(q)}(m)}{(X_{n-1}^2(m))^q} \tag{B3}$$

The recursion of Eq. B1 for X_n alone will as before converge to some distribution $P^*(X)$ satisfying Eq. A7. in the delocalized phase, one expects that the variables $C^{(q)}$ will grow exponentially (see Eqs 82). We thus set

$$D_n^{(q)} = e^{n\lambda_q} d^{(q)} \tag{B4}$$

where $\lambda_q > 0$ governs the exponential growth and where $d^{(q)}$ remains a finite random variable upon the iteration

$$e^{\lambda_q} d^{(q)} = \sum_{m=1}^{K} \frac{d^{(q)}(m)}{(X^2(m))^q} \tag{B5}$$

The similarity with the discussions of Appendix A is now obvious (see Eqs A4 and A5). Assuming the power-law decay

$$P^*(X, d) \underset{d \to \infty}{\simeq} \frac{\Phi(X)}{d^{1+\mu}} \tag{B6}$$

with $0 < \mu < 1$, one finds that the function $\Phi(X)$ has to satisfy the eigenvalue problem

$$e^{\mu \lambda_q} \Phi(X) = K \int \frac{dX_1}{(X_1^2)^{q\mu}} Q(X + \frac{1}{X_1}) \Phi(X_1) \tag{B7}$$

i.e. it is the same integral kernel as in Eq. A13 with the correspondences $\beta \to q\mu$ and $e^{-v\beta} \to e^{\mu \lambda_q}$, but now we are interested in the phase $\lambda_q > 0$.

2. Selection of tail exponents

We have argued above (see section A 6) that the problem for the function $\Phi(X)$ is well defined only for $0 < \beta = q\mu < 1/2$, i.e. the exponent μ_q that governs the power-law of Eq. B6 is restricted to the interval

$$0 < \mu_q < \frac{1}{2q} \tag{B8}$$

Denoting as before $\Lambda_0(\beta, W)$ the maximal eigenvalue of the kernel of Eq. A15, each mode μ is associated to the Lyapunov exponent (see Eq. A4)

$$\lambda_q(\mu) = \frac{1}{\mu} \ln \Lambda_0(q\mu, W) \tag{B9}$$

From Eq. A16, we have the following behavior for $\mu \to 0$

$$\lambda_q(\mu) \underset{\mu \to 0}{\simeq} \frac{1}{\mu} \ln K \tag{B10}$$

Near the other boundary $\mu \to 1/(2q)$, the property of Eq. A32, yields that the partial derivative with respect to μ is still negative at $\mu \to 1/(2q)$

$$[\partial_\mu \lambda_q(\mu)]_{\mu \to 1/(2q)} = \left[-\frac{1}{\mu^2} \ln \Lambda_0(1/2, W) \right]_{\mu \to 1/(2q)} < 0 \tag{B11}$$
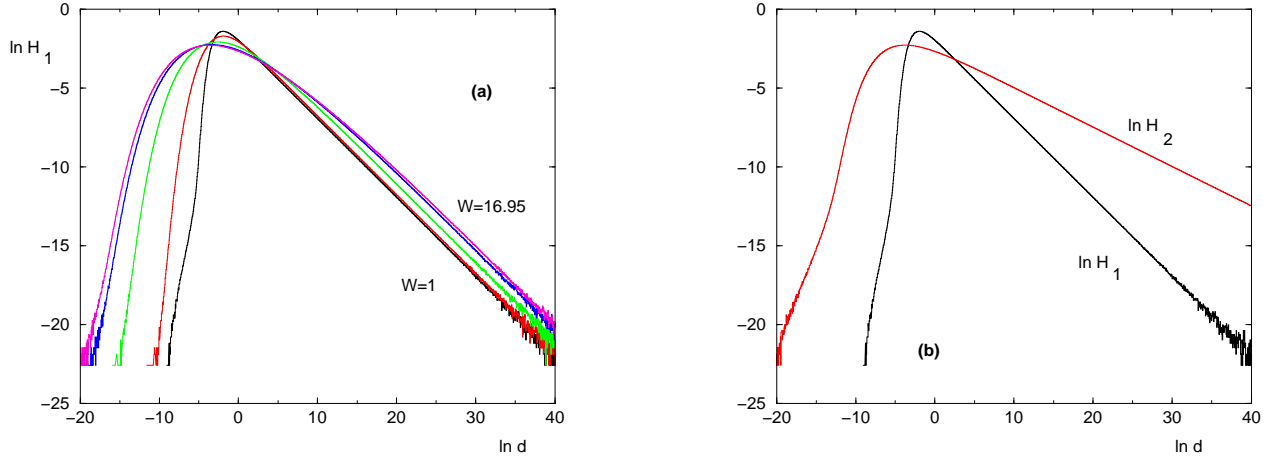
FIG. 12: (a) Probability distribution H_1 of the variable $\ln d^{(q=1)}$ of Eq. B4 for various disorder strength $W = 1, 5, 10, 15, 16.95$: the exponent μ_1^{selec} of Eq. B6 is of order $\mu_1^{selec} \sim 0.5$ in the whole delocalized phase. (b) For $W = 1$, comparison of the probability distributions H_1 and H_2 of the variable $\ln d^{(q)}$ for $q = 1$ and $q = 2$: the exponents of Eq. B6 are respectively $\mu_1^{selec} \sim 0.5$ and $\mu_2^{selec} \sim 0.25$ in agreement with Eq. B12.

For the special case $q = 1$, the curve $\lambda_1(\beta)$ is directly related via $\lambda_1(\beta) = -v(\beta)$ to the curve $v(\beta)$ discussed in Appendix A and shown on Fig. 11 (see the delocalized case $W < W_c$). Since the selected tail exponent μ_{selec} has to extremize $\lambda_q(\mu)$, we conclude that the selected tail exponents are given by the simple values

$$\mu_q^{selec} = \left(\frac{1}{2q}\right)^{-} \tag{B12}$$

in the whole delocalized phase. This is in agreement with our numerical results. We show on Fig. 12 (a) the probability distribution of $H_{q=1}(\ln d)$ of the variable $(\ln d)$ of Eq. B4 for various disorder strength $W = 1, 5, 10, 15, 16.95$: the tail exponent μ_1^{selec} of Eq. B6 remains of order $\mu_1^{selec} \sim 0.5$. For $q = 2$, we find similarly that the selected tail exponent remains the same within the whole delocalized phase and that it is of order $\mu_2^{selec} \sim 0.25$. On Fig. 12 (b), we compare for $W = 1$ the probability distributions $H_{q=1}(\ln d)$ and $H_{q=2}(\ln d)$ of the variables $\ln d^{(q=1)}$: the exponents of Eq. B6 are respectively $\mu_1^{selec} \sim 0.5$ and $\mu_2^{selec} \sim 0.25$.

From Eq. B12, we obtains that the Lyapunov exponents satisfy the identities

$$\lambda_q^{selec} = q\lambda_1^{selec} \tag{B13}$$

As explained in the text around Eq. 85, this identity is important to understand the decay of I.P.R. with the number N of generations in the delocalized phase.

3. Finite-size corrections introduced by the pool method

As explained in section II C 1, the pool method consists in representing a probability distribution $P(x)$ by a large number M_{pool} of random variables $\{x_i\}$. In particular this introduces a cut-off in the tail of $P(x)$ around x_{max} with $P(x_{max}) \sim 1/M_{pool}$. In the field of traveling waves, the presence of such a cut-off has been much studied (see [43] and references therein) : the leading correction to the selected velocity is usually logarithmic in M_{pool}

$$v_{selec}(M_{pool}) - v_{selec}(\infty) \sim \frac{J}{(\ln M_{pool})^{\alpha}} \tag{B14}$$

For our present problem, where the critical point corresponds to a vanishing velocity $v = 0$, we thus expect that the true critical point $W_c(\infty)$ corresponding to $v_{selec}(\infty) = 0$ will be shifted towards a pool-dependent pseudo-critical point $W_c(M_{pool})$ corresponding to $v_{selec}(M_{pool}) = 0$. As explained in the text, all the traveling waves encountered in the present paper vanish linearly in $(W - W_c)$. We thus expect that the difference $[W_c(M_{pool}) - W_c(\infty)]$ will also decay only logarithmically as $1/(\ln M_{pool})^{\alpha}$. From the analysis presented in Appendix A and B, it is obvious that the pool dependent critical point for the traveling wave of the Landauer transmission (see Appendix A) and for the

auxiliary variable $C^{(1)}$ or $D^{(1)}$ (see Appendix B) are the same because they are defined by the same condition in terms of the eigenvalue $\Lambda_0(\beta)$ of the integral kernel. However, the other variables $C^{(q)}$ or $D^{(q)}$ that have the same true critical point $W_c(\infty)$, will not have the same pool-dependent critical point $W_c(M_{pool})$, because the constant J in Eq. B14 will depend on q. This is indeed what we observe with our numerical computations with the pool $M_{pool} = 10^5$: the pseudo-critical point $W_c(M_{pool})$ for the variable $C^{(2)}$ is below the pseudo-critical point $W_c(M_{pool})$ for the variable $C^{(1)}$. We observe that the difference between the two becomes smaller for the bigger pool $M_{pool} = 10^6$. In conclusion, numerical studies based on the pool method are valid for observables that are related to a single traveling wave, but one cannot study the critical properties of observables that depend on two distinct traveling waves that have different pseudo-critical points. This is why in the text, we have not been able to present reliable numerical results for the statistics of I.P.R. I_2 that depends on both $C^{(1)}$ and $C^{(2)}$.

APPENDIX C: REMINDER ON THE TRAVELING/NON-TRAVELING PHASE TRANSITION STUDIED IN REF. [30]

In this Appendix, we briefly recall the finite-size scaling properties of the traveling/non-traveling phase transition studied in Ref. [30], because these properties are useful to interpret our numerical results described in the text.

For a one-dimensional branching random walk in the presence of an absorbing wall moving at a constant velocity v, the survival probability $Q(x,t)$ presents a phase transition at $v = v_v$ with the following critical behaviors (see more details in [30]) :

(i) for $v < v_c$, it converges exponentially in time towards a finite limit $Q^*(x) > 0$

$$Q(x,t) \simeq Q^*(x) + e^{-\frac{t}{\tau}} \phi(x) \tag{C1}$$

where the limit $Q^*(x)$ presents an essential singularity

$$Q^*(x) \simeq e^{-\frac{cte}{(v_c - v)^\kappa}} \quad \text{with} \quad \kappa = \frac{1}{2} \tag{C2}$$

and where the relaxation time τ diverges as

$$\tau \propto \frac{1}{(v_c - v)^\nu} \quad \text{with} \quad \nu = \frac{3}{2} \tag{C3}$$

(ii) for $v > v_c$, it converges exponentially in time towards zero

$$Q(x,t) \simeq e^{-\frac{t}{\tilde\tau}} \tag{C4}$$

where the relaxation time $\tilde\tau$ diverges as

$$\tilde\tau \propto \frac{1}{(v_c - v)^{\tilde\nu}} \quad \text{with} \quad \tilde\nu = 1 \tag{C5}$$

(iii) exactly at criticality, it converges towards zero with a stretched exponential

$$Q(x,t) \simeq e^{-(cte)t^\rho} \quad \text{with} \quad \rho = \frac{1}{3} \tag{C6}$$

(iv) the critical region is described by some finite-size scaling form governed by the relaxation time τ that appears in Eq. C1 (and not by the relaxation time $\tilde\tau$ appearing in Eq. C4)

$$\ln Q(x,t) \simeq -t^\rho G\left(t^{1/\nu}(v_c - v)\right) \tag{C7}$$

where the scaling function $G(u)$ has the following asymptotic behaviors. For $u \to +\infty$, has the one has the power-law

$$G(u) \underset{u \to +\infty}{\simeq} u^{-\nu\rho} \tag{C8}$$

to recover the finite limit of Eq. C2 and one has the scaling relation

$$\kappa = \nu\rho \tag{C9}$$

For $u \to -\infty$, one has the power-law

$$G(u) \underset{u \to -\infty}{\simeq} (-u)^{\nu(1-\rho)} \tag{C10}$$

to recover the exponential decay of Eq. C4, and one has the scaling relation

$$\tilde{\nu} = \nu(1 - \rho) \tag{C11}$$

For the problem considered in [30] all the exponents are exactly known $\tilde{\nu} = 1$, $\nu = 3/2$, $\rho = 1/3$ and $\kappa = 1/2$.

In our numerical results presented in the text concerning the traveling/non-traveling phase transitions that occur in Anderson localization on the Bethe lattice, we find very similar critical behaviors : the velocity of the traveling wave vanishes linearly with $\tilde{\nu} = 1$, and the finite-size scaling in the critical region is governed by the other exponent ν that appears in the relaxation towards the finite value of the non-traveling phase.

---

[1] P.W. Anderson, Phys. Rev. 109, 1492 (1958).
[2] D.J. Thouless, Phys. Rep. 13, 93 (1974) ; D.J. Thouless, in "Ill Condensed Matter" (Les Houches 1978), Eds R. Balian *et al.* North-Holland, Amsterdam (1979).
[3] B. Souillard, in " Chance and Matter" (Les Houches 1986), Eds J. Souletie *et al.* North-Holland, Amsterdam (1979) (1987).
[4] I.M. Lifshitz, S.A. Gredeskul and L.A. Pastur, "Introduction to the theory of disordered systems" (Wiley, NY, 1988).
[5] B. Kramer and A. MacKinnon, Rep. Prog. Phys. 56, 1469 (1993).
[6] P. Markos, Acta Physica Slovaca 56, 561 (2006).
[7] F. Evers and A.D. Mirlin, arXiv:0707.4378 to appear in Rev. Mod. Phys.
[8] E. Abrahams, P.W. Anderson, D.C. Licciardello and T.V. Ramakrishnan, Phys. Rev. Lett. 42, 673 (1979).
[9] R. Abou-Chacra, P.W. Anderson and D.J. Thouless, J. Phys. C : Solid State Physics 6, 1734 (1973) (see also R. Abou-Chacra and D. J. Thouless, J. Phys. C: Solid State Phys. 7, 65 (1974)).
[10] H. Kunz and B. Souillard, J. Physique Lettres 44, L411 (1983).
[11] A.D. Mirlin and Y.V. Fyodorov, Nucl. Phys. B 366, 507 (1991).
[12] M.R. Zirnbauer, Phys. Rev. B 34, 6394 (1986).
[13] J.J.M. Verbaarschot, Nucl. Phys. B300, 263 (1988).
[14] K.B. Efetov and O. Viehweger, Phys. Rev. B 45, 11546 (1992)
[15] K.B. Efetov, "Supersymmetry in disorder and chaos", Cambridge University Press (1997).
[16] B. Derrida and G.J. Rodgers, J. Phys. A : Math. Gen. 26, L457 (1993).
[17] J.D. Miller and B. Derrida, J. Stat. Phys. 75, 357 (1994).
[18] B. Shapiro, Phys. Rev. Lett. 50, 747 (1983).
[19] J.T. Chalker and S. Siak, J. Phys. : Condens. Matt. 2, 2671 (1990)
[20] P.M. Bell and A. MacKinnon, J. Phys. : Condens. Matt. 6, 5423 (1994).
[21] D.M. Basko, I.L. Aleiner, B.L. Altshuler, Annals of Physics 321, 1126 (2006) and Phys. Rev. B 76, 052203 (2007).
[22] B.L. Altshuler, Y. Gefen, A. Kamenev and L.S. Levitov, Phys. Rev. Lett. 78, 2803 (1997).
[23] P.G. Silvestrov, Phys. Rev. B 64, 113309 (2001).
[24] I.V. Gornyi, A.D. Mirlin and D.G. Polyakov, Phys. Rev. Lett. 95, 206603 (2005).
[25] V. Oganesyan and D.A. Huse, Phys. Rev. B 75, 155111 (2007).
[26] B. Derrida and H. Spohn, J. Stat. Phys. 51, 817 (1988).
[27] S.N. Majumdar and P.L. Krapivsky, Phys. Rev. E 62, 7735 (2000); S.N. Majumdar and P.L. Krapivsky, Phys. Rev. E 65, 036127 (2002) S.N. Majumdar and P.L. Krapivsky, Physica A 318, 161 (2003); S.N. Majumdar, Phys. Rev. E 68, 026103 (2003).
[28] U. Ebert and W. van Saarloos, Physica D 146, 1 (2000); W. van Saarloos, Phys. Rep. 386, 29 (2003).
[29] E. Brunet, Research lecture on the stochastic Fisher-KPP front equation (Marseille 2007), available at http://www.lps.ens.fr/ ebrunet/.
[30] B. Derrida and D. Simon, EPL 78, 60006 (2007); D. Simon and B. Derrida, J. Stat. Phys. 131, 203 (2008); D. Simon, PhD Thesis (2008), available at http://tel.archives-ouvertes.fr/tel-00286612/fr/
[31] R. Landauer, Philos. Mag. 21, 863 (1970).
[32] P. W. Anderson, D. J. Thouless, E. Abrahams and D. S. Fisher Phys. Rev. B 22, 3519 (1980).
[33] P. W. Anderson and P.A. Lee, Suppl. Prog. Theor. Phys. 69, 212 (1980).
[34] J.M. Luck, "Systèmes désordonnés unidimensionnels" , Alea Saclay (1992).
[35] A.D. Stone and A. Szafer, IBM J. Res. Dev. 32, 384 (1988).
[36] J. Prior, A.M. Somoza and M. Ortuno, Phys. Rev. B 72, 024206 (2005); A.M. Somoza, J. Prior and M. Ortuno, Phys. Rev. B 73, 184201 (2006); A.M. Somoza, M. Ortuno and J. Prior, Phys. Rev. Lett. 99, 116602 (2007).
[37] M. Sade and R. Berkovits, Phys. Rev. B 68, 193102 (2003).
[38] J.R. Banavar and A.J. Bray, Phys. Rev. B 35, 8888 (1987); M. Nifle and H.J. Hilhorst, Phys. Rev. Lett. 68 , 2992 (1992); T. Aspelmeier, A.J. Bray and M.A. Moore, Phys. Rev. Lett. 89, 197202 (2002).

[39] J. Cook and B. Derrida, J. Stat. Phys. 57, 89 (1989).

[40] C. Monthus and T. Garel, Phys. Rev. E 77, 021132 (2008); C. Monthus and T. Garel, Phys. Rev. B 77, 134416 (2008).

[41] A. Klein, Comm. Math. Phys. 177, 755 (1996).

[42] C. Monthus and C. Texier J. Phys. A: Math. Gen. 29 (1996) 2399.

[43] E. Brunet and B. Derrida, Phys. Rev. E 56, 2597 (1997); E. Brunet, B. Derrida, J. Stat. Phys. 103, 269 (2001); E. Brunet, B. Derrida, Phys. Rev. E 70, 016106 (2004); E. Brunet, B. Derrida, A. H. Mueller, S. Munier, Europhys. Lett., 76, 1 (2006); E. Brunet, B. Derrida, A. H. Mueller, and S. Munier; Phys. Rev. E 73, 056126 (2006); E. Brunet, B. Derrida, A. H. Mueller, and S. Munier Phys. Rev. E 76 041104 (2007).

[44] A.D. Mirlin and Y.V. Fyodorov, Phys. Rev. B 56, 13393 (1997).

[45] A.D. Mirlin and Y.V. Fyodorov, Phys. Rev. Lett. 72, 526 (1994); A.D. Mirlin and Y.V. Fyodorov, J. Phys. I France 4, 655 (1994).

[46] J. Brndiar and P. Markos, Phys. Rev. B 77, 115131 (2008).

[47] F. Evers and A.D. Mirlin, Phys. Rev. Lett. 84 , 3690 (2000) ; A.D. Mirlin and F. Evers, Phys. Rev. B 62, 7920 (2000).

[48] A. Mildenberger, F. Evers, and A. D. Mirlin Phys. Rev. B 66, 033109 (2002).

[49] C. Monthus and T. Garel, Phys. Rev. E 75, 051122 (2007).

[50] C. Monthus and T. Garel, Phys. Rev. E 75, 051119 (2007).

[51] R. H. McKenzie, Phys. Rev. Lett. 77, 4804 (1996); L. Balents and M. P. A. Fisher, Phys. Rev. B 56, 12970 (1997).

[52] F. Igloi and C. Monthus, Phys. Rep. 412, 277 (2005).